Università degli Studi di Bologna

FACOLTÀ DI INGEGNERIA

CORSO DI DOTTORATO IN MECCANICA APPLICATA ALLE MACCHINE
XVI CICLO

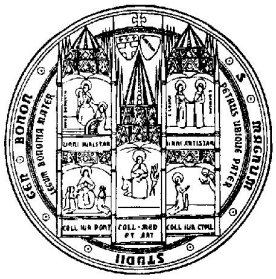

Methods for Clearance Influence Analysis in Planar and Spatial Mechanisms

Tesi di Dottorato di:

Stefano Venanzi

Coordinatore:

Chiar.mo Prof. **Vincenzo Parenti Castelli**

Tutore:

Chiar.mo Prof. **Vincenzo Parenti Castelli**

2004

Contents

Abstract

This doctoral dissertation presents a new method to asses the influence of clearance in the kinematic pairs on the configuration of planar and spatial mechanisms. The subject has been widely investigated in both past and present scientific literature, and is approached in different ways: a static/kinetostatic way, which looks for the clearance take-up due to the external loads on the mechanism; a probabilistic way, which expresses clearance-due displacements using probability density functions; a dynamic way, which evaluates dynamic effects like the actual forces in the pairs caused by impacts, or the consequent vibrations.

This dissertation presents a new method to approach the problem of clearance. The problem is studied from a purely kinematic perspective. With reference to a given mechanism configuration, the pose (position and orientation) error of the mechanism link of interest is expressed as a vector function of the degrees of freedom introduced in each pair by clearance: the presence of clearance in a kinematic pair, in facts, causes the actual pair to have more degrees of freedom than the theoretical clearance-free one. The clearance-due degrees of freedom are bounded by the pair geometry. A proper modelling of clearance-affected pairs allows expressing such bounding through analytical functions. It is then possible to study the problem as a maximization problem, where a continuous function (the pose error of the link of interest) subject to some constraints (the analytical functions bounding clearance-due degrees of freedom) has to be maximize.

Revolute, prismatic, cylindrical, and spherical clearance-affected pairs have been analytically modelled; with reference to mechanisms involving such pairs, the solution to the maximization problem has been obtained in a closed form.

Sommario

L'attività di ricerca presentata nella tesi di dottorato concerne lo studio dell'influenza del gioco nelle coppie cinematiche in meccanismi piani e spaziali. Tale tema è stato spesso oggetto di studi, tanto nella letteratura scientifica passata quanto in quella attuale. Da uno studio approfondito, si possono dedurre diverse metodologie per affrontare il problema: metodologie di tipo statico/cinetostatico, che determinano la ripresa nel gioco nelle coppie a seguito dell'azione di un carico; metodologie di tipo probabilistico, che esprimono lo spostamento nelle coppie con gioco in termini di funzioni densità di probabilità; infine, metodologie che si interessano al problema dinamico, volte a determinare effetti quali le effettive forze nelle coppie, o gli urti successivi al distacco e le conseguenti vibrazioni.

La tesi in oggetto presenta una nuova metodologia per affrontare il problema. Tale metodologia differisce dalle precedenti poiché presenta un'analisi di tipo puramente cinematico. Con riferimento ad una configurazione assegnata per un meccanismo, l'errore di posizione del membro di riferimento viene espresso come funzione vettoriale dei gradi di libertà introdotti dal gioco. La presenza di gioco in una coppia, infatti, introduce gradi di libertà aggiuntivi; questi gradi di libertà sono però vincolati. Un'opportuna modellazione delle coppie cinematiche affette da gioco permette di esprimere analiticamente per mezzo di opportune funzioni il vincolo sui gradi di libertà introdotti. E' quindi possibile studiare la funzione che rappresenta l'errore di posizionamento del membro di riferimento riconducendo il problema alla massimizzazione di una funzione continua definita su un dominio compatto. La soluzione al problema è ottenuta analiticamente in forma chiusa, modellando coppie di tipo rotoidale, prismatico, cilindrico e sferico per meccanismi piani e spaziali.

Introduction

The modelling of clearance in lower kinematic pairs is an old problem, and a lot of authors in time have proposed solutions based on different approaches. Even today, none of the proposed solutions can be univocally judged superior the others and adopted as standard. On the contrary, the different way to approach the problem is still visible in the scientific literature: each approach has its own strength points, and is suitable for solving a given class of problems, but not for giving a general answer.

From a chronological point of view, the clearance problem has been first addressed as a *kinematic* problem. Aim of the authors is the position analysis of clearance-affected mechanisms, that is the determination of the actual pose (position and orientation) of each link after the introduction of clearance in the pairs. However, such a position analysis strongly depends on the clearance take-up, and therefore on the forces acting in the pairs: the analysis analysis has then to include a static (or kinetostatic) analysis, and a purely kinematic analysis is not sufficient. The kinematic and static/kinetostatic analyses need models describing the clearance-affected pairs: such models have to map the relation between the pair forces and the clearance take-up. They depend on the kind of pair, and on the kind of mechanisms the pair belongs to (planar or spatial). When planar mechanisms are involved, planar models are sufficient to describe the pair. A simple model describing planar clearance-affected revolute pairs exists. Such a model is usually referred to as *equivalent clearance link* model. It introduces a fictitious massless link in the pair, which connects the pin center to the hole center in the pair (see Fig. 1). The fictitious link is assumed to display along the force direction to represent clearance take-up. The equivalent clearance link model is very widespread, and is universally accepted as representative for planar clearance-affected revolute pairs [1, 2, 3, 4]. The use of

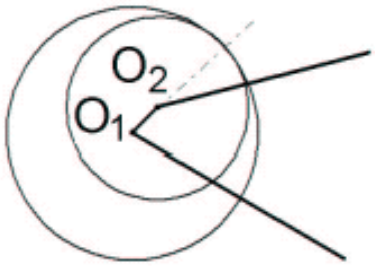

Figure 1: Equivalent clearance link

this model provides the clearance-due displacement in the pair as a function of the pair forces. After such a displacement is known, the clearance-affected mechanism becomes an ordinary mechanism, and its position analysis can be performed with standard techniques. To increase the accuracy, it is possible to perform the analysis in an iterative way. First, the pair forces are determined in a given configuration; then, the pair displacements are determined as a function of the pair forces, and a new configuration is achieved. After that, the pair forces can be re-determined in the new configuration, and an updated value of the pair displacements can be evaluated. In this way, a loop is built converging to the actual configuration of the clearance-affected mechanism [3].

Generalizing the equivalent clearance link to spatial mechanisms in not a trivial task. The model can be easily adapted for clearance-affected spherical pairs [4, 5]; however, other commonly used pairs, like the revolute or the prismatic ones, need more complex models. Furthermore, such models strongly depend on the actual pair design, as different designs define different take-up motions. Some kinetostatic models for the clearance-affected revolute pair in the form of journal bearing are presented in [6, 7, 8, 9]. The journal bearing design has been chosen because of its diffusion, and because it always needs clearance to work. In [10], a kinetostatic model is presented for prismatic pairs with a given design. All kinetostatic models provide the clearance-due displacement in the pairing elements as a function of the force in the pair: after the displacement in the pair is known, it can be used to perform the position analysis of the mechanism. In [7], the case of a spatial 4-bar linkage is presented. Regardless of the simple mechanism (only 4 pairs, and 4 links including the ground), the mathematics involved is very complex to handle, and not intuitive at all. For this reason, most of the authors choose a different

method to deal with spatial mechanisms: instead of an ordinary position analysis, a "displacement" analysis is performed. The hypothesis behind this approach concerns the magnitude of clearance: when small (theoretically infinitesimal) displacements are involved, it is much easier to analyze the ordinary clearance-free mechanism, and to find the pose error of its links caused by clearance, rather than analyzing the clearance-affected mechanism. Finding the position error can be considered a velocity analysis, rather than a position analysis. In this way, a complex non-linear problem (the position analysis of a clearance-affected mechanism) is replaced by an easier, well known non-linear problem (the position analysis of a clearance-free mechanism) and by a linear problem (the displacement/velocity analysis of a clearance-affected mechanism). The hypothesis of small values for clearance is usually fulfilled by real mechanisms, and such method is often followed for both open- [11, 12] and closed-chain mechanisms [9, 13, 14, 15, 16].

The approach based on kinematics and statics/kinetostatics at the same time solves the clearance problem in an efficient way, but has a major disadvantage: it basically depends on the load acting on the mechanism. It can be useful when working on mechanisms whose working conditions are precisely determined, but cannot perform the analysis of clearance-affected mechanisms working with unknown loads. Moreover, it cannot cope with effects like the loss of contact in the pairs. More generally, it involves statics/kinetostatics, and not kinematics only: as a consequence, it is not suitable for a general kinematic analysis of clearance-affected mechanisms. To account for this, some authors have replaced this deterministic approach with a *probabilistic* one [17, 18, 19]. Instead of kinetostatic models for the clearance-affected pairs, they use probability density functions expressing the displacement of the pairing elements. In this way, the displacements in clearance-affected pairs are expressed in a way which does not depend on the load, and no static/kinetostatic analysis is needed. After expressing the displacement in the pairs, the authors determine how such probability error functions propagate from the clearance-affected pairs to the output. Most of the times, a linear propagation model is used. The advantage of the probabilistic approach lies in its simplicity, and in the fact that other effects can be modelled in the same way (e.g., geometric tolerances on the links). However, it does not look deeply into the contact kinematics of the pair, and can be hardly associated with the physical side of the problem.

Another way to address the problem is the *dynamic* approach. Such approach does not focus on kinematics only; on the contrary, it considers the actual motion of the mechanism from a dynamic point of view. It can be used to obtain kinematic results, such as the trajectory of a mechanism link, or to evaluate completely different effects, like the actual forces in the joints, the loss of contact in the clearance affected pairs, the impacts between the pairing elements when the contact is re-established, or the impact frequency and the consequent vibrations. This approach can be based either on experimental results [20, 21], or on computer simulations. Computer simulations have been developed first for planar mechanisms [18, 22, 23, 24], for which the dynamic models have been enhanced to include link flexibility [25, 26]. The increased availability of computational resources in the last years could allow its extension to the spatial case; to the author's knowledge, however, only simple spatial mechanisms have been modelled until now [5].

The dynamic approach has the advantage of a very detailed modelling, suitable for finding almost all information about moving mechanisms. Unfortunately, it has a number of disadvantages. It is a very complex modelling, and requires simulation and integration in time: it is then time-consuming, both in the modelling and in the analysis. The results are strongly influenced by factors like boundary conditions, or assumptions on post-impact dynamics, and sometimes even by numerical factors such as the integration method or the integration step. As a result, it becomes a very specific, low-level tool, which needs testing and validation, and does not allow for a general approach to the problem.

In the last years, some authors have tried to develop a purely *kinematic* approach to the problem. Such an approach aims at a general, high level analysis of mechanisms from a purely kinematic point of view. In [4], the authors replace clearance-affected mechanisms with ordinary, underconstrained mechanisms. After that, they use workspace generation techniques to investigate the workspace of the new mechanisms in given configurations, and consider the workspace dimension as a parameter expressing clearance influence.

In what follows, a new method assessing the influence of clearance will be presented. The method is purely kinematic, and does not require knowledge of the load acting on the mechanism. In order to work, it needs kinematic models describing the displacement in the pairs. Analytical models for the most common pairs (revolute,

prismatic, cylindrical, spherical) are presented in detail. The method can be applied to both open- and closed-chain mechanisms. It is presented first for planar mechanism [27], and is then generalized to the case of spatial mechanisms. It provides the maximum pose error for the mechanism link of interest. When the mechanism pairs can be modelled analytically, the solution to the maximization problem is provided in a closed-form, granting that all possible solutions are found. Moreover, it is provided in a form which can be easily implemented with high numerical efficiency.

Chapter 1

Small Displacements Kinematics

The problem of assessing the influence of clearance in the pairs on mechanisms consists of two main points:

- determining the displacement between the pairing elements of each clearance-affected pair;
- determining how such a displacement affects the overall mechanism configuration.

The first point requires detailed models of the clearance-affected pairs; such models are reported in the following chapters. This chapter will tackle the second point, and a kinematic relation between the pair displacements and those of the overall mechanism will be achieved.

The most common method to perform the position analysis of mechanisms relies on Denavit-Hartenberg matrices [28, 29]. Such matrices are used do describe the significative geometry of each link (*geometry matrices*), and to describe the degrees of freedom of each pair(*pair matrices*). By properly combining the geometry and pair matrices, it is possible to obtain a non-linear equation system, usually referred to as *loop closure equations*. The solution of such a system determines the value of all degrees of freedom in the pairs, and gives then a solution to the position analysis.

The Denavit-Hartenberg modelling can be extended to account for clearance in the kinematic pairs. If a preliminary static/kinetostatic analysis is performed on the mechanism, it is possible to determine the constraint forces in clearance-affected joints, and, consequently, the displacement between the pairing elements

due to clearance take-up. The Denavit-Hartenberg matrices can then be modified, to express both the theoretical degree(s) of freedom in the pair, and the clearance-due displacement [7].

The solution of the "standard" loop closure equation is not a trivial task; it becomes even more difficult when clearance has to be considered. For this reason, other methods have been developed to assess the kinematic effects of clearance. All these methods rely on the assumption that clearance is small when compared to the other geometric dimensions. This hypothesis is usually fulfilled by industrial mechanisms, as designers tend to prescribe small values of clearance to make pairs work correctly. When clearance is small, its effects - that is, the generalized displacements it causes to the mechanism links after the actuators are locked - can be reasonably approximated by virtual displacements. In this way, the problem of solving the position analysis for a clearance-affected mechanism is replaced by two easier problems:

1. First, solving the position analysis for the clearance-free mechanism, and determining its theoretical configuration;

2. Then, estimating the displacement of its links caused by clearance take-up.

This approach has been used in [11] and [12] to study serial mechanisms, that is, mechanisms whose links form an open kinematic chain. Since the mechanism is serial, all pairs have to be actuated: the pair nominal degree of freedom (the rotation about the pair axis) is given. However, the presence of clearance in the pair gives raise to a generalized displacement between the pairing elements. To express such a displacement, it is convenient to introduce two reference systems, one fixed to each element. The systems are chosen so that one overlaps the other when clearance is not taken-up. After clearance take-up, the two systems do not overlap any more (see Fig. 1.1). A relative translation has displaced the two origins 0 and $0'$. Such translation, $\overline{t}$, is a 3-component vector, and will be called *translation error*. Furthermore, a change in the relative orientation has occurred. The change in orientation can be thought as a relative rotation between the two systems, and represented by a vector $\overline{r}$ with direction parallel to the line of rotation and magnitude equal to the rotation angle. According to Euler's theorem, $\overline{r}$ exists and is unique; it will be referred to as *rotation error*. Since the rotation about the pair axis is controlled, $\overline{r}$ is orthogonal

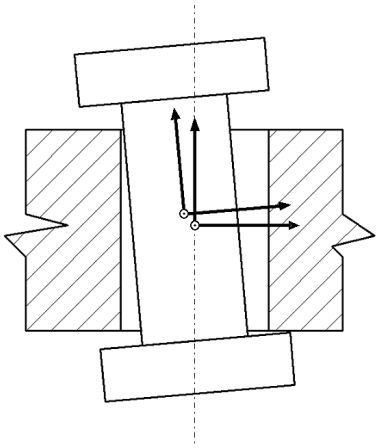

Figure 1.1: Translation and rotation error

to the pair axis.

Both translation and rotation errors have a direct effect on the relative positioning of the links. If a point A_i is assumed on the i-th link, its displacement with respect to link $i-1$, $\overline{A}_{i,i-1}$, caused by the clearance-affected pair, is

$$\Delta\overline{A}_{i,i-1} = \overline{t}_{i,i-1} + \overline{r}_{i,i-1} \times (\overline{A}_i - \overline{O}_i) \tag{1.1}$$

whereas the change of orientation $\Delta\overline{\Psi}_{i,i-1}$ of link i with respect to link $i-1$ is

$$\Delta\overline{\Psi}_{i,i-1} = \overline{r}_{i,i-1} \tag{1.2}$$

When all clearance-affected revolute pairs are considered at the same time, all effects can be superimposed because of the linearity of instantaneous kinematics. Eqs. (1.1) and (1.2) become then

$$\Delta\overline{A}_{n,0} = \sum_{i=1}^{n} \overline{t}_i + \sum_{i=1}^{n} \overline{r}_i \times (\overline{A}_n - \overline{O}_i) \tag{1.3}$$

and

$$\Delta\overline{\Psi}_{n,0} = \sum_{i=1}^{n} \overline{r}_i \tag{1.4}$$

where $A_{n,0}$ is the point on link n whose displacement is being sought, O_i is the origin of the reference system on the i-th clearance-affected pair, while $\overline{t}_i$ and $\overline{r}_i$ are its translation and rotation error. The two equations are still valid when pairs other than revolute are considered; only, the definition of $\overline{t}$ and $\overline{r}$ has to be properly adjusted: for a prismatic pair, $\overline{t}$ will be orthogonal to the pair geometric axis; for

a cylindrical pair, both $\overline{t}$ and $\overline{r}$ will be orthogonal to the pair axis; for a spherical pair, $\overline{r}$ will be null.

This vectorial approach presents several strength points. It is numerically very efficient, as it requires vector algebra only instead of matrices. The kinematic composition of small displacements is very intuitive from a geometric perspective. Moreover, this way of geometrically obtaining the displacement of a link is consistent with other techniques used to analyze manipulators: when the clearance-due displacements are replaced by the unitary motion of the ideal pair, the elements in Eqs. (1.3) and (1.4) can be properly arranged to evaluate the Jacobian matrix for the manipulator; when the displacements are replaced by vectors representing geometric inaccuracies, they can assess the influence of such an error on the pose of a link.

Unfortunately, Eqs. (1.3) and (1.4) hold for serial mechanisms only. When closed kinematic chains are considered, the problem becomes more complex. In [13], the authors generalize Eqs. (1.3) and (1.4) to the case of closed-loops. First, they consider the kinematic composition of angular and linear velocity. The angular velocity of link i with respect to link j is given by

$$\overline{\omega}_{i,j} = \sum_{k=i}^{j} \overline{\omega}_{k,k-1} \tag{1.5}$$

where $\overline{\omega}_{k,k-1}$ is the angular velocity of link k with respect to link $k-1$. Similarly, the linear velocity of point $\overline{A}_i$ (on link i) with respect of point $\overline{A}_j$ (on link j) is

$$\overline{v}_{i,j} = \sum_{k=i}^{j} \overline{v}_{k,k-1} + \sum_{k=i}^{j} \overline{\omega}_{k,k-1} \times (\overline{A}_k - \overline{A}_{k-1}) \tag{1.6}$$

where A_k and A_{k-1} are two representative points on links k and $k-1$ respectively, while $v_{k,k-1}$ is the linear velocity of point A_{k-1}.

Equations (1.5) and (1.6) can be used to relate the errors caused by clearance: when such errors are small, they can be considered as virtual displacement, and can therefore replace velocities. Moreover, when the loop closure is considered, and all links (from 0 to n) are taken into account, Eqs. (1.5) and (1.6) become

$$\Delta\overline{\Psi}_{n,0} = \sum_{k=0}^{n} \Delta\overline{\Psi}_{k,k-1} = \overline{0} \tag{1.7}$$

$$\Delta\overline{A}_{n,0} = \sum_{i=0}^{n} \Delta\overline{A}_{k,k-1} + \sum_{i=0}^{n} \overline{\Psi}_{k,k-1} \times (\overline{A}_k - \overline{A}_{k-1}) = \overline{0} \tag{1.8}$$

Equations (1.7) and (1.8) are a set of 2 vector (6 scalar) equations relating the changes in orientation between two connected links, $\Delta\Psi_{k,k-1}$, and the change in position between some representative points on two connected links, $\Delta A_{k,k-1}$. Both changes in orientation and position are due in part to clearance take up, and in part to the degrees of freedom of the idle pairs that have to adapt to the clearance take-up. If the clearance take-up is somehow determined, e.g. through a static/kinetostatic analysis, it is possible to use Eqs. (1.7) and (1.8) to determine the motion in the idle pairs, and then determine the pose error (and indirectly the mechanism configuration). More generally, the two equations relate the displacement in the clearance-affected pairs with that of the mechanism links. When more than one loop exists, one set of equations has to be written for every loop.

This approach is as general as the previous one, and works for both open and closed chains. It could also be generalized to model other error sources, like the geometric inaccuracies. When the displacements caused by the controlled dofs are considered instead of those caused by clearance, the solution of Eqs. (1.7) and (1.8) can be used to evaluate the Jacobian matrix relating output and input variables for the mechanism.

A different way to obtain equations similar to (1.7) and (1.8) is presented in [9] and [16]. Instead of the kinematic composition of both angular and linear velocity, the authors use the duality between statics and instantaneous kinematics. The mechanism link of interest, that is the link whose clearance-due displacement is sought, is loaded by a virtual load $\overline{G}$. The virtual load can be a generalized load: in that case it can be dealt with as a 6-component vector, 3 components to represent a force, 3 components to represent a moment. A static analysis of the ideal clearance-free mechanism provides the (generalized) pair forces, $\overline{S}_i$. Similarly to the generalized load, the pair forces $\overline{S}_i$ can be considered as 6-component vectors. When the mechanism actuators are locked, the mechanism behaves like a fully constrained structure (isostatic structure), and a linear relation exists between $\overline{G}$ and each of the pair forces $\overline{S_i}$. The linear relation can be expressed as

$$\overline{S}_i = \mathbf{H_i}\overline{G} \tag{1.9}$$

where $\mathbf{H_i}$ is a 6x6 matrix whose elements depend on the mechanism configuration only. Matrix $\mathbf{H_i}$ can be easily obtained with 6 static analysis: the first one, performed with a load $\overline{G}_1 = [1\ 0\ 0\ 0\ 0\ 0]^T$, provides its first column; the second, performed with $\overline{G}_2 = [0\ 1\ 0\ 0\ 0\ 0]^T$, provides its second column, and so on until $\overline{G}_6 = [0\ 0\ 0\ 0\ 0\ 1]^T$ provides its last column.

When virtual generalized displacements $\overline{\Delta\gamma_i}$ are introduced between the pairing elements of n clearance-affected pairs, a virtual generalized displacement $\overline{\Delta\Gamma}$ arises on the link of interest. The principle of virtual work can be used to relate all the displacements; it allows writing the equation

$$\overline{G}^T\overline{\Delta\Gamma} + \sum_{i=1}^{n} \overline{S}_i^T\overline{\Delta\gamma_i} = 0 \tag{1.10}$$

which can be re-arranged as

$$\overline{G}^T\overline{\Delta\Gamma} + \sum_{i=1}^{n} \overline{G}^T\mathbf{H_i}^T\overline{\Delta\gamma_i} = 0 \tag{1.11}$$

Since Eq. (1.11) holds regardless of the load, G can be dropped, thus providing

$$\overline{\Delta\Gamma} = -\sum_{i=1}^{n} \mathbf{H_i}^T\overline{\Delta\gamma_i} \tag{1.12}$$

Similarly to Eqs. (1.7) and (1.8), Eq. (1.12) is a purely kinematic relation between the generalized displacement in the clearance-affected pairs, $\Delta\gamma_i$, and that of the link of interest, $\Delta\Gamma$. The kinematic relation is based on matrices $\mathbf{H_i}$. Such matrices map the static relation between load and pair forces; their transpose maps the kinematic relation between the displacements associated with those forces.

The kinematic relation expressed by Eq. (1.12) is almost the same as that in Eqs. (1.7) and (1.8). It is as general, and could also be used to include other error sources. It has the advantage of directly providing the displacement of the link of interest, and it consists of 6 scalar equations regardless of the number of loops involved. Furthermore, its formulation can be used in the same way for both open and closed chain mechanisms.

In what follows, the kinematic analysis of clearance-affected mechanisms will be performed. The last technique in this chapter will be used to perform the analysis; however, all the techniques previously reviewed could be used indifferently.

Chapter 2

Clearance in Planar Mechanisms

In this chapter, the study of clearance influence is presented for planar mechanisms. Because of their simplicity, such mechanisms are commonly used for a number of tasks. For the same reason, clearance effects have been extensively studied in the literature. Different authors have presented both kinematic and dynamic models, up to different detail levels. The clearance model presented here is a high level, very simplified model. It gives a general overview of the mechanism from a kinematic perspective, and can be very useful to compare different design solutions. Moreover, it can be considered as the key to better understand the modelling of spatial mechanisms, presented in next chapter.

2.1 Pose Error Function

When working in the plane, a rigid body can have up to three degrees of freedom (dofs). Two of them concern its position in the plane - translation dofs; the third one concerns its orientation - rotation dof. When all actuators of a clearance-free mechanism are locked, the three dofs are determined for every link. This is not true for clearance-affected mechanism: because of clearance take-up, the links are allowed a limited motion. The limited motion of the mechanism link of interest will be called from here on *position error*. It can be represented by the 3-component vector $\Delta\Gamma$

$$\Delta\Gamma = \begin{bmatrix} \Delta X \\ \Delta Y \\ \Delta\Theta \end{bmatrix} \tag{2.1}$$

with two translation components, ΔX and ΔY and one rotation component, $\Delta\Theta$.

A similar definition applies to the clearance-affected pairs. Theoretically, such pairs allow one (or two) dof(s) between the pairing elements; when the actuators are locked, those dofs are uniquely assigned. Because of clearance, however, a relative motion between the pairing elements exists. The relative motion between the elements of the i-th pair will be referred to as $\Delta\gamma_i$, and called *local displacement*. Similarly to Eq. (2.1), it can be represented by a 3-component vector:

$$\Delta\gamma_i = \begin{bmatrix} \Delta x_i \\ \Delta y_i \\ \Delta\theta_i \end{bmatrix} \tag{2.2}$$

with two translation components, Δx_i and Δy_i and one rotation component, $\Delta\theta_i$.

A kinematic relation exists between $\Delta\Gamma$ and $\Delta\gamma_i$. When clearance magnitude is much smaller than the link size, it can be expressed by Eqs. (1.3) and (1.4), (1.7) and (1.8), or (1.12). As previously explained, Eq. (1.12) will be used from here on, that is

$$\Delta\Gamma = -\sum_{i=1}^{n} \mathbf{H_i}^T \Delta\gamma_i \quad (1.12\ \textit{repeated}) \tag{2.3}$$

where n is the number of clearance-affected pairs, and $\mathbf{H_i}$ are known matrices obtained through the static analysis of the clearance-free mechanism. Since a planar mechanism is considered, they are 3x3 matrices.

Equation (2.3) provides the pose error $\Delta\Gamma$ as a function of some unknown parameters, the local displacements $\Delta\gamma_i$ and, consequently, of their components Δx_i, Δy_i, and $\Delta\theta_i$. In order to determine the pose error, it is sufficient to study such a function. To do this, a proper definition of the local displacements is first needed.

2.2 Pair Modelling

The definition of the local displacements $\Delta\gamma_i$ basically depends on the kind of pair considered. The most common pairs are the revolute and the prismatic one.

2.2.1 Revolute pair

A clearance-free revolute pair allows a relative rotation between the pairing elements, bounding all relative translations. On the contrary, the presence of clearance permits

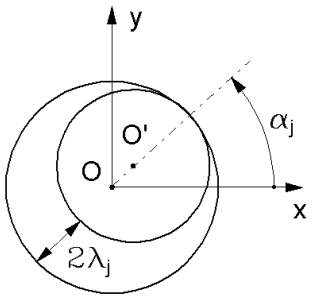

Figure 2.1: Revolute Pair

the relative translation between the pairing elements. With reference to Fig. 2.1, the local displacement $\Delta\gamma_i$ can be expressed as

$$\Delta\gamma_i = \begin{bmatrix} \rho_i \cos(\alpha_i) \\ \rho_i \sin(\alpha_i) \\ 0 \end{bmatrix} \tag{2.4}$$

The rotation component has a null value, because the relative rotation between the elements is not caused by clearance but belongs to the pair dofs. The two translation components are expressed in the coordinate system shown in Fig. 2.1, whose origin lies on the theoretical pair center. They are expressed as functions of two parameters, ρ_i and α_i, reported in Fig. 2.1. The numerical definition of the parameters uniquely identifies the relative positioning of the pairing elements. The two parameters cannot assume any value but are constrained by the pair design: ρ_i, the distance between the pin and the hole center, has to be equal to or smaller than the clearance value. This can be easily expressed by

$$0 \leq \rho_i \leq \epsilon \tag{2.5}$$

where ϵ is clearance magnitude. When ρ_i is equal to the clearance value, the pin is in contact with the hole on a point whose angular position is defined by the parameter α_i. When ρ_i is smaller than the clearance value, the pin is floating with respect to the hole.

2.2.2 Prismatic Pair

A clearance-free prismatic pair allows the translation along one direction between the pairing elements; the translation along the other direction and the relative rotation

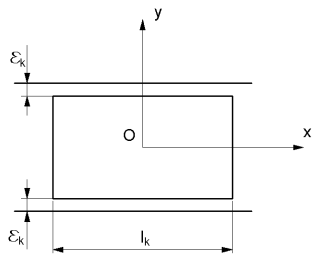

Figure 2.2: Prismatic Pair

are constrained. Clearance allows these last two dofs. With reference to Fig. 2.2, the displacement $\Delta\gamma_j$ is

$$\Delta\gamma_j = \begin{bmatrix} 0 \\ \sigma_j \\ \tau_j \end{bmatrix} \tag{2.6}$$

σ_j and τ_j are two parameters: σ_j associated with a translation orthogonal to the pair geometrical axis, and τ_j represents the relative rotation. The translation along the pair geometrical axis is not present in $\Delta\gamma_j$ because it belongs to the ideal pair, and is not caused by clearance. The numerical definition of σ_j and τ_j uniquely defines the relative position between the pairing elements. The values of σ_j and τ_j are bounded by the pair design. After $\Delta\gamma_i$ is applied to the slider, the y-displacement of its corner points (point A, B, C, and D in Fig. 2.2) has to be equal to or smaller than the value of clearance. This determines the four constraints

$$\begin{cases} L\sin(\tau_j) + d\cos(\tau_j) + 2\sigma_j - d - 2\epsilon \leq 0 \\ -L\sin(\tau_j) + d\cos(\tau_j) + 2\sigma_j - d - 2\epsilon \leq 0 \\ -L\sin(\tau_j) - d\cos(\tau_j) + 2\sigma_j + d + 2\epsilon \geq 0 \\ L\sin(\tau_j) - d\cos(\tau_j) + 2\sigma_j + d + 2\epsilon \geq 0 \end{cases} \tag{2.7}$$

For the sake of clarity, it is convenient to represent the inequalities (2.7) in a graphic way. In a σ_j - τ_j plane, the inequalities define the internal part of a [concave] diamond - see Fig. 2.3. When the hypothesis of small clearance is used, the inequalities (2.7) are simplified to

$$\begin{cases} L\tau_j + 2\sigma_j - 2\epsilon \leq 0 \\ -L\tau_j + 2\sigma_j - 2\epsilon \leq 0 \\ -L\tau_j + 2\sigma_j + 2\epsilon \geq 0 \\ L\tau_j + 2\sigma_j + 2\epsilon \geq 0 \end{cases} \tag{2.8}$$

and the sides of the diamond in Fig. 2.3 become straight lines.

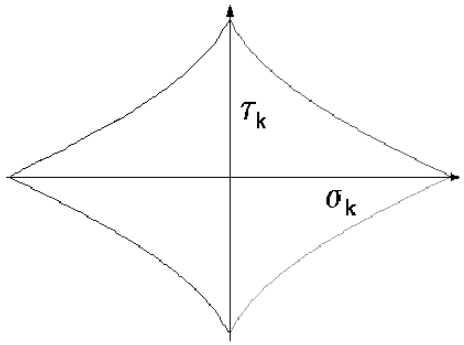

Figure 2.3: Constraints on σ_j and τ_j

2.3 Study of the Pose Error

The definition of the local displacements (2.4) and (2.6) when plugged into Eq. (2.3) defines the pose error as a function of the unknown parameters describing the contact in the pairs: α_i and ρ_i for each revolute pair, σ_j and τ_j for each prismatic pair. Because of the structure of Eq. (2.3), based on the hypothesis of small values for clearance, each component of the pose error is

- a linear trigonometric function when revolute-pair parameters appear;
- a linear function when prismatic-pair parameters appear.

The pose error has the form

$$\Delta\Gamma = \begin{bmatrix} ...\mathbf{H_i}_{1,1}\rho_i\cos(\alpha_i) + \mathbf{H_i}_{1,2}\rho_i\sin(\alpha_i) + ... + \mathbf{H_j}_{1,2}\sigma_j + \mathbf{H_j}_{1,3}\tau_j + ... \\ ...\mathbf{H_i}_{2,1}\rho_i\cos(\alpha_i) + \mathbf{H_i}_{2,2}\rho_i\sin(\alpha_i) + ... + \mathbf{H_j}_{2,2}\sigma_j + \mathbf{H_j}_{2,3}\tau_j + ... \\ ...\mathbf{H_i}_{3,1}\rho_i\cos(\alpha_i) + \mathbf{H_i}_{3,2}\rho_i\sin(\alpha_i) + ... + \mathbf{H_j}_{3,2}\sigma_j + \mathbf{H_j}_{3,3}\tau_j + ... \end{bmatrix} \quad (2.9)$$

where $\mathbf{H_i}_{a,b}$ represents the element in the a-th row, b-th column in matrix $\mathbf{H_i}$. It is possible to study each component of the pose error, in order to determine its maximum and minimum value. Such a study is simplified by the fact that each component is a linear function, thus.

- the maxima/minima exist, and lie on the domain border;
- the function can be split in n parts, where n is the number of clearance-affected pairs. Each part can be dealt with separately, to find its maximum/minimum; the global maximum/minimum will be the sum of all the maxima/minima for the different pairs.

The numerical procedures to find the maximum/minimum for revolute and prismatic pairs are hereafter reported.

2.3.1 Revolute Pair

When the q-th component of the pose error $\Delta\Gamma$ given by Eq. (2.9) is considered, the contribution of the i-th clearance affected revolute pair is

$$f = \mathbf{H}_{\mathbf{i}q,1}\rho_i \cos(\alpha_i) + \mathbf{H}_{\mathbf{i}q,2}\rho_i \sin(\alpha_i) \tag{2.10}$$

The function f is subject to the constraint

$$0 \leq \rho_i \leq \epsilon \tag{2.11}$$

where ϵ is clearance magnitude. Since the maxima/minima lie on the domain border, it is

$$\rho_i = \epsilon \tag{2.12}$$

The values of α_i generating maxima/minima can be obtained by the condition

$$\partial f/\partial\alpha_i = 0 \tag{2.13}$$

which yields

$$\begin{aligned} \alpha_{i_1} &= \arctan(\mathbf{H}_{\mathbf{i}q,2}/\mathbf{H}_{\mathbf{i}q,1}) \\ \alpha_{i_2} &= \arctan(\mathbf{H}_{\mathbf{i}q,2}/\mathbf{H}_{\mathbf{i}q,1}) \pm \pi \end{aligned} \tag{2.14}$$

where one of the two values of α_i generates a maximum, the other one generates a minimum.

2.3.2 Prismatic Pair

When the q-th component of the pose error $\Delta\Gamma$ given by Eq. (2.9) is considered, the contribution of the j-th clearance affected revolute pair is

$$f = \mathbf{H}_{\mathbf{j}q,2}\sigma_j + \mathbf{H}_{\mathbf{j}q,3}\tau_j \tag{2.15}$$

The variables σ_j and τ_j are subject to the constraints

$$\begin{cases} L\sin(\tau_j) + d\cos(\tau_j) + 2\sigma_j - d - 2\epsilon \leq 0 \\ -L\sin(\tau_j) + d\cos(\tau_j) + 2\sigma_j - d - 2\epsilon \leq 0 \\ -L\sin(\tau_j) - d\cos(\tau_j) + 2\sigma_j + d + 2\epsilon \geq 0 \\ L\sin(\tau_j) - d\cos(\tau_j) + 2\sigma_j + d + 2\epsilon \geq 0 \end{cases} \tag{2.16}$$

Table 2.1: Mechanism dimensions

Dimensions	value
OB	10
AC	40
CD	10
AO	25
h	20

where ϵ is the magnitude of clearance. The constraints are graphically shown in Fig. 2.3. Since f is a linear function defined on a concave domain, its maxima/minima are generated on the domain vertices. It means that f can have a maximum/minimum in one of the four points

$$\begin{aligned} \sigma_j = +\epsilon \quad \tau_j = 0 \\ \sigma_j = -\epsilon \quad \tau_j = 0 \\ \sigma_j = 0 \quad \tau_j = +\arctan(\tfrac{dL+2\epsilon L-d\sqrt{L^2-4d\epsilon-4\epsilon^2}}{d^2+2d\epsilon+L\sqrt{L^2-4d\epsilon-4\epsilon^2}}) \\ \sigma_j = 0 \quad \tau_j = -\arctan(\tfrac{dL+2\epsilon L-d\sqrt{L^2-4d\epsilon-4\epsilon^2}}{d^2+2d\epsilon+L\sqrt{L^2-4d\epsilon-4\epsilon^2}}) \end{aligned} \tag{2.17}$$

Using the hypothesis of small clearance, Eq. (2.17) becomes

$$\begin{aligned} \sigma_j = +\epsilon \quad \tau_j = 0 \\ \sigma_j = -\epsilon \quad \tau_j = 0 \\ \sigma_j = 0 \quad \tau_j = +2\epsilon/L \\ \sigma_j = 0 \quad \tau_j = -2\epsilon/L \end{aligned} \tag{2.18}$$

After these four points have been found, the evaluation of f in these points permits finding its maximum/minimum value.

2.4 Numerical Example

In this section, the clearance influence analysis is applied to an ordinary quick-return mechanism. The mechanism is shown in Fig.2.4. The mechanism dimensions are reported in Table 2.1; all lengths are in arbitrary units (a.u.). The angular position of the crank OB, θ, is considered as the input, whereas the linear position of the slider - identified by the x-coordinate of point D, x_D - is the output. The input value $\theta = \frac{7}{8}\pi$ is chosen to perform the analysis. Once the crank angle θ is given,

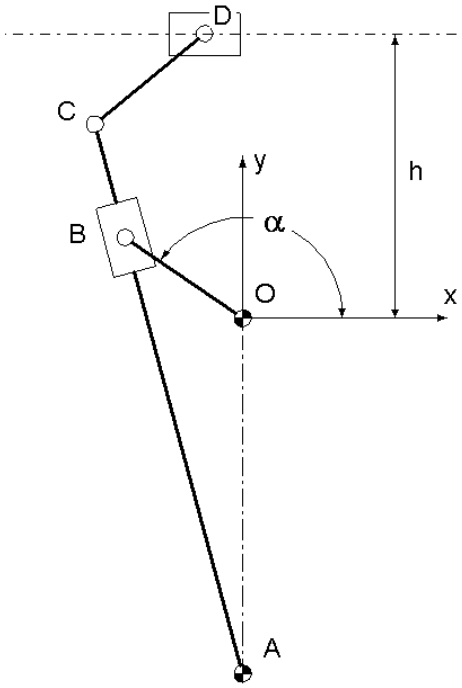

Figure 2.4: Ordinary quick-return mechanism

the position analysis provides two possible configurations for the mechanism. The configuration in Fig.2.4 is chosen; in such a configuration, $x_D = -4.9775$. All pairs are affected by clearance. Clearance magnitude is assumed to be 0.1 a.u. for both revolute and prismatic pairs. The dimensions of the slider in each prismatic pair have to be given to determine the maximum rotation τ; such dimensions are assumed to be 3 a.u. for the slider length (L in Fig. 2.2), 1 a.u. for the slider transverse dimension (d in Fig. 2.2).

Three virtual static analyses of the mechanism provide matrices **H**. The first virtual analysis is performed with a load $G_1 = [1\ 0\ 0]^T$, that is with a force along the x-direction. The force is applied to point D. This analysis provides the first column of all matrices **H**. The second analysis is performed with a virtual load $G = [0\ 1\ 0]^T$, that is with a force directed along the y-axis and applied to point D. It provides the second column of all matrices **H**. The third analysis is performed with a virtual load $G = [0\ 0\ 1]^T$, that is with a moment acting on the slider. It provides the third

column of each matrix $\mathbf{H}$. The final result is:

$$\mathbf{H_1} = \begin{bmatrix} +1.5653 & 0 & 0 \\ +0.5017 & 0 & 0 \\ 0 & 0 & 0 \end{bmatrix}$$

for the revolute pair in O;

$$\mathbf{H_2} = \begin{bmatrix} -0.5653 & 0 & 0 \\ +0.4539 & 0 & 0 \\ 0 & 0 & 0 \end{bmatrix}$$

for the revolute pair in A;

$$\mathbf{H_3} = \begin{bmatrix} +1.5653 & 0 & 0 \\ +0.5017 & 0 & 0 \\ 0 & 0 & 0 \end{bmatrix}$$

for the revolute pair in B;

$$\mathbf{H_4} = \begin{bmatrix} +1.5653 & 0 & 0 \\ +0.5017 & 0 & 0 \\ 0 & 0 & 0 \end{bmatrix}$$

for the prismatic pair in B;

$$\mathbf{H_5} = \begin{bmatrix} +1 & 0 & 0 \\ +0.9555 & 0 & 0 \\ 0 & 0 & 0 \end{bmatrix}$$

for the revolute pair in C;

$$\mathbf{H_6} = \begin{bmatrix} +1 & 0 & 0 \\ +0.9555 & 0 & 0 \\ 0 & 0 & 0 \end{bmatrix}$$

for the revolute pair in D;

$$\mathbf{H_7} = \begin{bmatrix} 0 & 0 & 0 \\ -0.9555 & 1 & 0 \\ 0 & 0 & 1 \end{bmatrix}$$

for the prismatic pair in D. All matrices are expressed in the reference system shown in Fig. 2.4.

The local displacements for the revolute pairs are

$$\Delta\gamma_i = \begin{bmatrix} \rho_i \cos(\alpha_i) \\ \rho_i \sin(\alpha_i) \\ 0 \end{bmatrix}$$

with $i = 1, 2, 3, 5, 6$. These displacements are related to the revolute pairs in O, A, B, C, and D respectively. The local displacement for the prismatic pair in B, expressed in the coordinate system in Fig. 2.4, is

$$\Delta\gamma_4 = \begin{bmatrix} 0.9523\sigma_4 \\ 0.3052\sigma_4 \\ \tau_4 \end{bmatrix}$$

while the local displacement in the prismatic pair in D, expressed in the same coordinate system, is

$$\Delta\gamma_7 = \begin{bmatrix} 0 \\ \sigma_7 \\ \tau_7 \end{bmatrix}$$

It is now possible to use (Eq. 2.3) to obtain the function describing the slider pose error. The function has 3 components: the first two are the $x-$ and $y-$displacement of point D; the third one is the slider rotation. The pose error function is

$$\Delta\Gamma = \begin{bmatrix} \Delta X = \begin{array}{c} +1.5653 \cdot \rho_1 \cos(\alpha_1) + 0.5017 \cdot \rho_1 \sin(\alpha_1) \\ -0.5653 \cdot \rho_2 \cos(\alpha_2) + 0.4539 \cdot \rho_2 \sin(\alpha_2) \\ +1.5653 \cdot \rho_3 \cos(\alpha_3) + 0.5017 \cdot \rho_3 \sin(\alpha_3) \\ +1.0000 \cdot \rho_5 \cos(\alpha_5) + 0.9555 \cdot \rho_5 \sin(\alpha_5) \\ +1.0000 \cdot \rho_6 \cos(\alpha_6) + 0.9555 \cdot \rho_6 \sin(\alpha_6) \\ +1.6437 \cdot \sigma_4 - 0.9555 \cdot \sigma_7 \end{array} \\ \\ \Delta Y = \sigma_7 \\ \\ \Delta\Theta = \tau_7 \end{bmatrix}$$

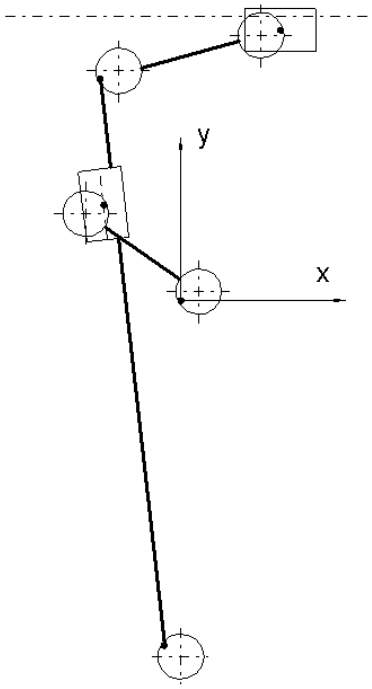

Figure 2.5: Ordinary quick-return mechanism affected by clearance: maximum error on the output slider position

The slider position error along the y-axis (ΔY) and its orientation error ($\Delta\Theta$) depend only on the clearance in the prismatic pair in D, whereas the slider position error along the x-axis (ΔX) depends on the clearance in all the pairs.

The study of the functions ΔX, ΔY and $\Delta\Theta$ provides the maximum errors affecting the slider caused by clearance. The numerical solution is:

1. For ΔX,

$$\begin{array}{rcrcl}
\rho_1 = 0.1 & \alpha_1 = \{0.3102; -2.8314\} & \Longrightarrow & \Delta X = \pm 0.1644 \\
\rho_2 = 0.1 & \alpha_2 = \{-0.6765; 2.4651\} & \Longrightarrow & \Delta X = \pm 0.0725 \\
\rho_3 = 0.1 & \alpha_3 = \{0.3102; -2.8314\} & \Longrightarrow & \Delta X = \pm 0.1644 \\
\sigma_4 = \pm 0.1 & \tau_4 = 0 & \Longrightarrow & \Delta X = \pm 0.1644 \\
\rho_5 = 0.1 & \alpha_5 = \{0.7626; -2.3789\} & \Longrightarrow & \Delta X = \pm 0.1383 \\
\rho_6 = 0.1 & \alpha_6 = \{0.7626; -2.3789\} & \Longrightarrow & \Delta X = \pm 0.1383 \\
\sigma_7 = \pm 0.1 & \tau_7 = 0 & \Longrightarrow & \Delta X = \pm 0.0956
\end{array}$$

$$\Longrightarrow \Delta X = \pm 0.9379$$

2. For ΔY,

$$\sigma_7 = \pm 0.1 \quad \tau_7 = 0 \quad \Longrightarrow \quad \Delta Y = \pm 0.1$$

$$\Longrightarrow \Delta Y = \pm 0.1$$

3. For $\Delta\Theta$,

$$\sigma_7 = 0 \quad \tau_7 = \pm 0.0668 \quad \Longrightarrow \quad \Delta\Theta = \pm 0.0668$$

$$\Longrightarrow \Delta\Theta = \pm 0.0668$$

Figure 2.5 reports the mechanism configuration associated with the maximum error on the slider position along the x-axis (the magnitude of clearance is amplified to show the contact conditions in the pairs).

Chapter 3

Spatial Clearance-Affected Mechanisms

The study of clearance influence presented in the previous chapter can be extended to the case of spatial mechanisms. The kinematic analysis of spatial clearance-affected mechanisms can be performed as for planar mechanisms. The only difference concerns the kinematic pairs. With spatial mechanisms, a wider variety of pairs can be used; furthermore, the kinematic behavior of the clearance-affected pairs is strongly influenced by the pair design, and its modelling is more complex.

In this chapter, the analysis of clearance influence is detailed for spatial mechanisms. After the definition of the pose error, the chapter focusses on the modelling of the most common pairs, and on the maximization of the pose error.

3.1 Pose Error Function

A rigid body has up to six degrees of freedom (dofs). Three concern its position - translation dofs; three concern its orientation - rotation dofs. When all actuators of a clearance-free mechanism are locked, the six dofs are determined for every link. However, the presence of clearance allows a limited link motion. The motion of the mechanism link of interest will be called from hereon *position error*, and referred to

as $\Delta\Gamma$. It can be represented by a 6-component vector,

$$\Delta\Gamma = \begin{bmatrix} \Delta X \\ \Delta Y \\ \Delta Z \\ \Delta\Xi \\ \Delta H \\ \Delta\Upsilon \end{bmatrix} \tag{3.1}$$

where ΔX, ΔY, and ΔZ represent the change in position of a reference point on the link of interest, while $\Delta\Xi$, ΔH, and $\Delta\Upsilon$ represent a change in the link orientation. When magnitude rotation is small, these last three parameters can be intended as the components of a vector; if the rotation creating the change in orientation is considered, such a vector has the same direction as the rotation axis, and the same magnitude as the rotation magnitude.

Clearance-affected pairs can be treated in a similar way: while clearance-free pairs constrain some dofs between the pairing element, clearance-affected pairs limit those dofs, but do not constrain them completely. They allow thus a relative displacement. Such displacement will be referred to as $\Delta\gamma_i$, and called *local displacement*. It can be represented by a 6-component vector,

$$\Delta\gamma_i = \begin{bmatrix} \Delta x_i \\ \Delta y_i \\ \Delta z_i \\ \Delta\xi_i \\ \Delta\eta_i \\ \Delta\upsilon_i \end{bmatrix} \tag{3.2}$$

where Δx_i, Δy_i, and Δz_i are associated with the linear displacement, and $\Delta\xi_i$, $\Delta\eta_i$, and $\Delta\upsilon_i$ are associated with the angular displacement.

A kinematic relation exists between $\Delta\Gamma$ and $\Delta\gamma_i$. When clearance magnitude is small, it can be expressed by one between Eqs. (1.3) and (1.4), (1.7) and (1.8), or (1.12). As previously explained, Eq. (1.12) will be used from here on:

$$\Delta\Gamma = -\sum_{i=1}^{n} \mathbf{H_i}^T \Delta\gamma_i \quad (1.12\ \textit{repeated}) \tag{3.3}$$

where n is the number of clearance-affected pairs, and $\mathbf{H_i}$ are known matrices, obtained through the static analysis of the clearance-free mechanism. Since spatial mechanisms are considered, they are 6x6 matrices.

Equation (3.3) provides the pose error $\Delta\Gamma$ as a function of some unknown parameters, the local displacements $\Delta\gamma_i$. In order to determine the pose error, it is sufficient to study such a function. In order to do that, a proper definition of the local displacements is first needed.

3.2 Pair Modelling

The local displacements $\Delta\gamma_i$ depend on the kind of pair, as different pairs define different relative motions, and, by converse, different displacements. Some common pairs are here revised.

3.2.1 Revolute Pair

A revolute pair allows one rotational dof only between the pairing elements. The local displacement $\Delta\gamma_i$ will then involve the components which are supposed to be bounded. If $\Delta\gamma_i$ is expressed in a reference system with z-axis along the pair axis, it can be defined as

$$\Delta\gamma_i = \begin{bmatrix} \Delta x_i \\ \Delta y_i \\ \Delta z_i \\ \Delta\xi_i \\ \Delta\eta_i \\ 0 \end{bmatrix} \tag{3.4}$$

Because of the cylindrical symmetry usual for revolute pairs, it is convenient to express $\Delta\gamma_i$ as

$$\Delta\gamma_i = \begin{bmatrix} \rho_i \cos(\phi_i) \\ \rho_i \sin(\phi_i) \\ \Delta z_i \\ \theta_i \cos(\psi_i) \\ \theta_i \sin(\psi_i) \\ 0 \end{bmatrix} \tag{3.5}$$

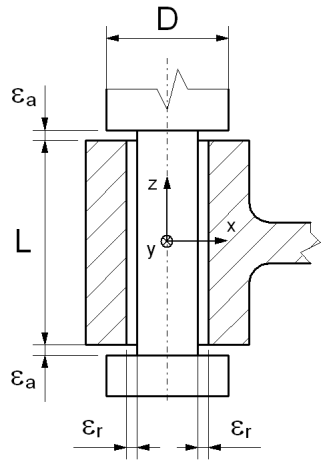

Figure 3.1: Journal bearing

where ρ_i, ϕ_i, θ_i, and ψ_i are parameters defining the relative displacement between the pairing elements. The value of such parameters is bounded by the geometry of the pairing elements; thus, it is necessary to refer to a specific design for the revolute pair. The journal bearing design reported in Fig. 3.1 is chosen. Such a design is common for revolute pairs; moreover, it always needs clearance in order to work. Two reference systems, each one fixed to one of the pairing elements, are taken; when clearance is not taken up, the two systems overlap and their origins lie on the theoretical pair center (see Fig. 3.1). $\Delta\gamma_i$ can be intended as the displacement between the two pairing elements, and its magnitude is bounded by the possible contact between the elements. The contact can occur in not more than four points:

1. on the upper rim of the hole;

2. on the lower rim of the hole;

3. on the upper shoulder;

4. on the lower shoulder.

The contact could also occur on one line and one plane; however, from a kinematic point of view, such a contact can be modelled exactly like a 3-point contact, with the two points on the rims belonging to the contact line.

When small displacements are considered, the displacement of a point on the upper rim is

$$\begin{bmatrix} \frac{L}{2}\theta_i \sin(\psi_i) + \rho_i \cos(\psi_i) \\ -\frac{L}{2}\theta_i \cos(\psi_i) + \rho_i \sin(\psi_i) \\ -\sin(\theta_i)\sin(\psi_i)\frac{d}{2}\cos(\alpha) + \sin(\theta_i)\cos(\psi_i)\frac{d}{2}\sin(\alpha) + \Delta z_i \end{bmatrix} \tag{3.6}$$

where d is the pin diameter, L is the pin length, and α identifies the point on the rim. The displacement component in a plane parallel to the xy-plane has to be smaller than the magnitude of radial clearance. This can be expressed by the inequality

$$\left(\frac{L}{2}\theta_i \sin(\psi_i) + \rho_i \cos(\psi_i)\right)^2 + \left(-\frac{L}{2}\theta_i \cos(\psi_i) + \rho_i \sin(\psi_i)\right)^2 \leq \epsilon_r^2 \tag{3.7}$$

where ϵ_r is the magnitude of radial clearance. Eq. (3.7) can be simplified to

$$\rho_i^2 + \frac{L^2}{4}\theta_i^2 + \rho_i \theta_i L \sin(\psi_i - \phi_i) \leq \epsilon_r^2 \tag{3.8}$$

The displacement of a point on the lower rim is

$$\begin{bmatrix} -\frac{L}{2}\theta_i \sin(\psi_i) + \rho_i \cos(\psi_i) \\ \frac{L}{2}\theta_i \cos(\psi_i) + \rho_i \sin(\psi_i) \\ -\sin(\theta_i)\sin(\psi_i)\frac{d}{2}\cos(\beta) + \sin(\theta_i)\cos(\psi_i)\frac{d}{2}\sin(\beta) + \Delta z_i \end{bmatrix} \tag{3.9}$$

where β identifies the point on the rim. The displacement component in a plane parallel to the xy-plane has to be smaller than the magnitude of radial clearance; this can be expressed by the inequality

$$\left(-\frac{L}{2}\theta_i \sin(\psi_i) + \rho_i \cos(\psi_i)\right)^2 + \left(\frac{L}{2}\theta_i \cos(\psi_i) + \rho_i \sin(\psi_i)\right)^2 \leq \epsilon_r^2 \tag{3.10}$$

which can be simplified to

$$\rho_i^2 + \frac{L^2}{4}\theta_i^2 - \rho_i \theta_i L \sin(\psi_i - \phi_i) \leq \epsilon_r^2 \tag{3.11}$$

The z-component displacement of a point on the upper shoulder is

$$\frac{D}{2}\theta_i \sin(\delta - \psi_i) + \Delta z_i \tag{3.12}$$

where D is the shoulder diameter, while δ identifies the point on the rim. Its maximum magnitude occurs for the point with $\delta = \psi_i + \frac{\pi}{2}$, and is

$$\frac{D}{2}\theta_i + \Delta z_i \tag{3.13}$$

This displacement has to be smaller than the value of axial clearance, ϵ_a, thus the following constraint function is obtained

$$\frac{D}{2}\theta_i + \Delta z_i \leq \epsilon_a \tag{3.14}$$

Similarly, the z-component displacement of a point on the lower shoulder is expressed by Eq. (3.12). Its minimum magnitude occurs when $\delta = \psi_i - \frac{\pi}{2}$, and is

$$-\frac{D}{2}\theta_i + \Delta z_i \tag{3.15}$$

This displacement has to be bigger (i.e. smaller in magnitude, but with negative sign) than the value of axial clearance, ϵ_a, thus the following constraint function is obtained

$$-\frac{D}{2}\theta_i + \Delta z_i \geq \epsilon_a \tag{3.16}$$

which becomes

$$\frac{D}{2}\theta_i - \Delta z_i \leq \epsilon_a \tag{3.17}$$

In summary, four constraint functions have been identified for a clearance-affected pair designed as a journal bearing. The four constraint functions are reported in the set (3.18), and reflect the possible contacts between the pairing elements. When the contact occurs on four points, they have to be considered at the same time. When the contact is on three point, only three of them have to be considered: as an example, if the contact occurs on the two rims and on the upper shoulder, only the first, the second and the third inequality in the set (3.18) have to be considered.

$$\begin{cases} \rho_i^2 + \frac{L^2}{4}\theta_i^2 + \rho_i\theta_i L\sin(\psi_i - \phi_i) \leq \epsilon_r^2 \\ \rho_i^2 + \frac{L^2}{4}\theta_i^2 - \rho_i\theta_i L\sin(\psi_i - \phi_i) \leq \epsilon_r^2 \\ \frac{D}{2}\theta_i + \Delta z_i \leq \epsilon_a \\ \frac{D}{2}\theta_i - \Delta z_i \leq \epsilon_a \end{cases} \tag{3.18}$$

3.2.2 Cylindrical Pair

A cylindrical pair allows the rotation about one axis and the translation along the same axis. The local displacement $\Delta\gamma_j$ involves the components which are supposed to be bounded: when $\Delta\gamma_j$ is expressed in a reference system with z-axis along the

pair axis, it can be defined as

$$\Delta\gamma_j = \begin{bmatrix} \Delta x_j \\ \Delta y_j \\ 0 \\ \Delta\xi_j \\ \Delta\eta_j \\ 0 \end{bmatrix} \tag{3.19}$$

Because of the cylindrical symmetry, it is convenient to express $\Delta\gamma_j$ as

$$\Delta\gamma_i = \begin{bmatrix} \rho_j \cos(\phi_j) \\ \rho_j \sin(\phi_j) \\ 0 \\ \theta_j \cos(\psi_j) \\ \theta_j \sin(\psi_j) \\ 0 \end{bmatrix} \tag{3.20}$$

where ρ_j, ϕ_j, θ_j, and ψ_j are parameters defining the displacement between the pairing elements. The value of such parameters is bounded by the geometry of the pairing elements. The design reported in Fig. 3.2 is chosen. The contact between the pairing elements is very similar to that of the revolute pair, and can occur on two points only (A and B in Fig. 3.2). Again, when the contact occurs on one line, it can be modelled by referring to the extremes of that line only.

When small displacements are considered, the displacement of point A is

$$\begin{bmatrix} \frac{L}{2}\theta_j \sin(\psi_j) + \rho_j \cos(\psi_j) \\ -\frac{L}{2}\theta_j \cos(\psi_j) + \rho_j \sin(\psi_j) \\ -\sin(\theta_j)\sin(\psi_j)\frac{d}{2}\cos(\alpha) + \sin(\theta_j)\cos(\psi_j)\frac{d}{2}\sin(\alpha) + \Delta z_j \end{bmatrix} \tag{3.21}$$

where d is the pin diameter, L is the pin length, and α identifies the point. The displacement component in a plane parallel to the xy-plane has to be smaller than the magnitude of radial clearance. This can be expressed by the inequality

$$\left(\frac{L}{2}\theta_j \sin(\psi_j) + \rho_j \cos(\psi_j)\right)^2 + \left(-\frac{L}{2}\theta_j \cos(\psi_j) + \rho_j \sin(\psi_j)\right)^2 \leq \epsilon_r^2 \tag{3.22}$$

where ϵ_r is the magnitude of radial clearance. Eq. (3.22) can be simplified to

$$\rho_j^2 + \frac{L^2}{4}\theta_j^2 + \rho_j\theta_j L \sin(\psi_j - \phi_j) \leq \epsilon_r^2 \tag{3.23}$$

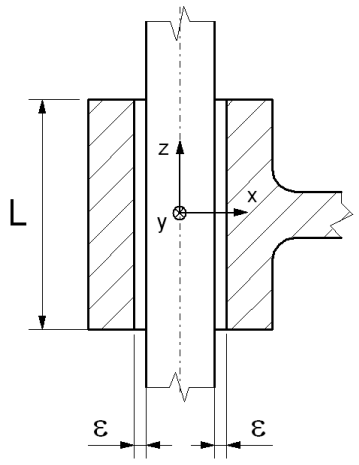

Figure 3.2: Cylindrical pair

The displacement of point B is

$$\begin{bmatrix} -\frac{L}{2}\theta_j \sin(\psi_j) + \rho_j \cos(\psi_j) \\ \frac{L}{2}\theta_j \cos(\psi_j) + \rho_j \sin(\psi_j) \\ -\sin(\theta_j)\sin(\psi_j)\frac{d}{2}\cos(\beta) + \sin(\theta_j)\cos(\psi_j)\frac{d}{2}\sin(\beta) \end{bmatrix} \tag{3.24}$$

where β identifies the point. The displacement component in a plane parallel to the xy-plane has to be smaller than the magnitude of radial clearance; this can be expressed by the inequality

$$\left(-\frac{L}{2}\theta_j \sin(\psi_j) + \rho_j \cos(\psi_j)\right)^2 + \left(\frac{L}{2}\theta_j \cos(\psi_j) + \rho_j \sin(\psi_j)\right)^2 \leq \epsilon_r^2 \tag{3.25}$$

which can be simplified to

$$\rho_j^2 + \frac{L^2}{4}\theta_j^2 - \rho_j \theta_j L \sin(\psi_j - \phi_j) \leq \epsilon_r^2 \tag{3.26}$$

In summary, two constraint functions have been identified for a clearance-affected cylindrical pair. The two constraint functions are reported in the set (3.27).

$$\begin{cases} \rho_j^2 + \frac{L^2}{4}\theta_j^2 + \rho_j \theta_j L \sin(\psi_j - \phi_j) \leq \epsilon_r^2 \\ \rho_j^2 + \frac{L^2}{4}\theta_j^2 - \rho_j \theta_j L \sin(\psi_j - \phi_j) \leq \epsilon_r^2 \end{cases} \tag{3.27}$$

3.2.3 Spherical Pair

A spherical pair constrains any translation between the pairing elements, while it allows any rotation. Thus, the local displacement $\Delta\gamma_k$ involves the translation components only. When $\Delta\gamma_j$ is expressed in a reference system with z-axis along the

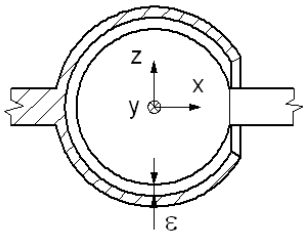

Figure 3.3: Spherical pair

pair axis, it can be defined as

$$\Delta\gamma_k = \begin{bmatrix} \Delta x_k \\ \Delta y_k \\ \Delta z_k \\ 0 \\ 0 \\ 0 \end{bmatrix} \tag{3.28}$$

Because of its symmetry, it is convenient to express $\Delta\gamma_k$ as

$$\Delta\gamma_i = \begin{bmatrix} \rho_k \cos(\phi_k)\cos(\psi_k) \\ \rho_k \sin(\phi_k)\cos(\psi_k) \\ \rho_k \sin(\psi_k) \\ 0 \\ 0 \\ 0 \end{bmatrix} \tag{3.29}$$

where ρ_k, ϕ_k, and ψ_k are parameters expressing the displacement between the pairing elements. The value of such parameters is bounded by the geometry of the pairing elements. The contact between the pairing elements can occur on one point only, and the displacement magnitude has to be smaller than clearance magnitude. This implies

$$\Delta x^2 + \Delta y^2 + \Delta z^2 \leq \epsilon^2 \tag{3.30}$$

or, by using Eq. (3.29),

$$0 \leq \rho_k \leq \epsilon \tag{3.31}$$

where ϵ is the magnitude of clearance.

3.2.4 Prismatic Pair

A prismatic pair allows one translational dof only between the pairing elements. The local displacement $\Delta\gamma_l$ will then involve the components which are supposed to be bounded. If $\Delta\gamma_l$ is expressed in a reference system with z-axis parallel to the translation axis, it can be defined as

$$\Delta\gamma_l = \begin{bmatrix} \Delta x_l \\ \Delta y_l \\ 0 \\ \Delta\xi_l \\ \Delta\eta_l \\ \Delta\zeta_l \end{bmatrix} \tag{3.32}$$

where x_l and y_l are parameters expressing the translation error, while ξ_l, η_l and ζ_l express the rotation error. The value of such parameters is bounded by the geometry of the pairing elements; thus, it is necessary to refer to a specific design for the revolute pair. The design reported in Fig. 3.4 has been chosen. Two reference systems, each one fixed with one of the pairing elements, are taken; their z-axis lies on the pair geometric axis, while the origin is in the pair geometric center (see Fig. 3.4). $\Delta\gamma_l$ can be intended as the displacement between the two pairing elements, and its magnitude is bounded by the possible contact between the elements. The contact can occur in eight different points, reported as P_n, $n = 1..8$, in Fig. 3.4. The coordinates of points P_n are

$$P_n = \begin{bmatrix} \pm a/2 \\ \pm a/2 \\ \pm l/2 \end{bmatrix} \tag{3.33}$$

where a is the pair lateral dimension, and l is the pair length. When small displacements are considered, the displacements of points P_n is

$$\Delta P_n = \begin{bmatrix} \pm\frac{l}{2}\Delta\eta_l \mp \frac{a}{2}\Delta\zeta_l + \Delta x_l \\ \mp\frac{l}{2}\Delta\xi_l \pm \frac{a}{2}\Delta\zeta_l + \Delta y_l \\ 0 \end{bmatrix} \tag{3.34}$$

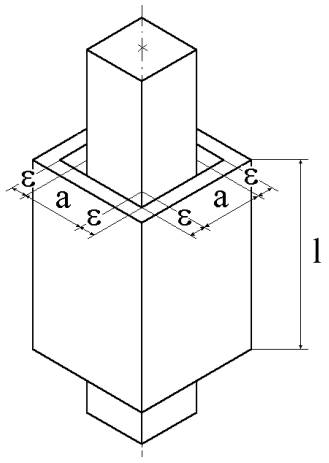

Figure 3.4: Prismatic pair

The x and y coordinates of ΔP_n have to be equal to or smaller than clearance magnitude ϵ, thus providing the inequalitiy set

$$\begin{cases} -l\Delta\eta_l - 2\Delta x_l - a\Delta\zeta_l \leq 2\epsilon & -l\Delta\xi_l - 2\Delta y_l - a\Delta\zeta_l \leq 2\epsilon \\ -l\Delta\eta_l - 2\Delta x_l + a\Delta\zeta_l \leq 2\epsilon & -l\Delta\xi_l - 2\Delta y_l + a\Delta\zeta_l \leq 2\epsilon \\ -l\Delta\eta_l + 2\Delta x_l - a\Delta\zeta_l \leq 2\epsilon & -l\Delta\xi_l + 2\Delta y_l - a\Delta\zeta_l \leq 2\epsilon \\ -l\Delta\eta_l + 2\Delta x_l + a\Delta\zeta_l \leq 2\epsilon & -l\Delta\xi_l + 2\Delta y_l + a\Delta\zeta_l \leq 2\epsilon \\ l\Delta\eta_l - 2\Delta x_l - a\Delta\zeta_l \leq 2\epsilon & l\Delta\xi_l - 2\Delta y_l - a\Delta\zeta_l \leq 2\epsilon \\ l\Delta\eta_l - 2\Delta x_l + a\Delta\zeta_l \leq 2\epsilon & l\Delta\xi_l - 2\Delta y_l + a\Delta\zeta_l \leq 2\epsilon \\ l\Delta\eta_l + 2\Delta x_l - a\Delta\zeta_l \leq 2\epsilon & l\Delta\xi_l + 2\Delta y_l - a\Delta\zeta_l \leq 2\epsilon \\ l\Delta\eta_l + 2\Delta x_l + a\Delta\zeta_l \leq 2\epsilon & l\Delta\xi_l + 2\Delta y_l + a\Delta\zeta_l \leq 2\epsilon \end{cases} \tag{3.35}$$

3.3 Study of the Pose Error

After the local displacements (3.5), (3.5), and (3.29) have been defined, their introduction into Eq. (2.3) defines the pose error as a function of the numerical parameters in the pairs: ρ_i, ϕ_i, Δz_i, θ_i, and ψ_i for each revolute pair; ρ_j, ϕ_j, θ_j, and ψ_j for each cylindrical pair; ρ_k, ϕ_k and ψ_k for each spherical pair; and Δx_l, Δy_l, $\Delta\xi_l$, $\Delta\eta_l$, and $\Delta\zeta_l$ for each prismatic pair. Because of the structure of Eq. (2.3),

the q-th component of the pose error has the form

$$\begin{aligned}\Delta\Gamma^q = &...\mathbf{H_i}_{q,1}\rho_i\cos(\phi_i) + \mathbf{H_i}_{q,2}\rho_i\sin(\phi_i) + \mathbf{H_i}_{q,3}\Delta z_i + \mathbf{H_i}_{q,4}\theta_i\sin(\psi_i)\\ &+\mathbf{H_i}_{q,5}\theta_i\sin(\psi_i) + ... + \mathbf{H_j}_{q,1}\rho_j\cos(\phi_j) + \mathbf{H_j}_{q,2}\rho_j\sin(\phi_j) + \mathbf{H_j}_{q,4}\theta_j\sin(\psi_j)\\ &+\mathbf{H_j}_{q,5}\theta_j\sin(\psi_j) + ...\mathbf{H_k}_{q,1}\rho_k\cos(\phi_k)\cos(\psi_k) + \mathbf{H_k}_{q,2}\rho_k\sin(\phi_i)\cos(\psi+k)\\ &+\mathbf{H_k}_{q,3}\rho_k\sin(\psi_k) + ... + \mathbf{H_l}_{q,1}\Delta x_l + \mathbf{H_l}_{q,2}\Delta y_l + \mathbf{H_l}_{q,4}\Delta\xi_l + \mathbf{H_l}_{q,5}\Delta\eta_l +\\ &+\mathbf{H_l}_{q,6}\Delta\zeta_l + ...\end{aligned} \tag{3.36}$$

Equation (3.36) is valid when all matrices $\mathbf{H}$ and displacements $\Delta\gamma$ are expressed in the same reference system. In general, however, the reference systems chosen to express $\Delta\gamma$ in the form of Eqs. (3.5), (3.20) and (3.29) are different. It is then convenient to introduce suitable matrices to change the coordinates from the local reference systems in the pairs to the global reference system in which matrices $\mathbf{H}$ have been obtained. Such matrices are 6x6 orthogonal matrices in the form

$$\mathbf{M_i} = \begin{bmatrix} \mathbf{R_i} & \mathbf{0} \\ \mathbf{0} & \mathbf{R_i} \end{bmatrix} \tag{3.37}$$

where $\mathbf{R_i}$ is the 3x3 rotational matrix that changes the coordinates between the local system of the i-th pair and the global coordinate system. Equation (3.36) takes thus the form

$$\begin{aligned}\Delta\Gamma^q = &...K_{i,1}\rho_i\cos(\phi_i) + K_{i,2}\rho_i\sin(\phi_i) + K_{i,3}\Delta z_i + K_{i,4}\theta_i\sin(\psi_i)\\ &+K_{i,5}\theta_i\sin(\psi_i) + ... + K_{j,1}\rho_j\cos(\phi_j) + K_{j,2}\rho_j\sin(\phi_j) + K_{j,4}\theta_j\sin(\psi_j)\\ &+K_{j,5}\theta_j\sin(\psi_j) + ...K_{k,1}\rho_k\cos(\phi_k)\cos(\psi_k) + K_{k,2}\rho_k\sin(\phi_i)\cos(\psi+k)\\ &+K_{k,3}\rho_k\sin(\psi_k) + ... + K_{l,1}\Delta x_l + K_{l,2}\Delta y_l + K_{l,4}\Delta\xi_l + K_{l,5}\Delta\eta_l +\\ &+K_{l,6}\Delta\zeta_l + ...\end{aligned} \tag{3.38}$$

where $K_{i,j}$ are numerical coefficients depending on $\mathbf{H_i}$ and $\mathbf{M_i}$.

Equation (3.38) is a continuous function of the parameters introduced to describe the pair displacement, and is defined on a limited domain. It is then possible to state that it has a maximum on its domain. Another interesting property is that there is no coupling between those parameters: no term contains two (or more) parameters referring to two (or more) different pairs. In this case, the function can be split in n sub-functions, one for each clearance-affected pair. The maximization of the entire function can then be replaced by the maximization of n simpler function, as the function maximum will be the sum of the maxima for all parts.

The maximization procedure is here reported for the pairs previously considered.

3.3.1 Revolute Pair

The sub-function concerning a revolute pair has the form

$$f = K_{i,1}\rho_i \cos(\phi_i) + K_{i,2}\rho_i \sin(\phi_i) + K_{i,3}\Delta z_i + K_{i,4}\theta_i \cos(\psi_i) + K_{i,5}\theta_i \sin(\psi_i) \quad (3.39)$$

subject to the constraints

$$\begin{cases} \rho_i^2 + \frac{L^2}{4}\theta_i^2 + \rho_i\theta_i L \sin(\psi_i - \phi_i) \leq \epsilon_r^2 \\ \rho_i^2 + \frac{L^2}{4}\theta_i^2 - \rho_i\theta_i L \sin(\psi_i - \phi_i) \leq \epsilon_r^2 \\ \frac{D}{2}\theta_i + \Delta z_i \leq \epsilon_a \\ \frac{D}{2}\theta_i - \Delta z_i \leq \epsilon_a \end{cases} \quad (3.40)$$

The maximum for f is to be looked for on the domain border; inside the domain, local maxima have to satisfy the condition ∇f=0, which leads to the system

$$\begin{cases} K_{i,1}\cos(\phi_i) + K_{i,2}\sin(\phi_i) = 0 \\ -K_{i,1}\rho_i \sin(\phi_i) + K_{i,2}\rho_i \cos(\phi_i) = 0 \\ K_{i,3} = 0 \\ K_{i,4}\cos(\psi_i) + K_{i,5}\sin(\psi_i) = 0 \\ -K_{i,4}\theta_i \sin(\phi_i) + K_{i,5}\theta_i \sin(\psi_i) = 0 \end{cases} \quad (3.41)$$

whose only solution gives a null value for both ρ_i and θ_i (provided the condition $K_{i,3} = 0$ is satisfied); such a solution is neither the function minimum nor its maximum. The domain border is defined by the constraints (3.40). In principle, all possible comibinations of the four constraint functions should be considered. From a physical point of view, however, the domain border is associated with the complete take-up of clearance. When clerance is completely taken-up, the contact between the pairing elements can occur

- on four points, two on the shoulders and two on the rims;
- on three points, two on the shoulders and one on one rim;
- on three points, one on one shoulder and two on the rims;
- on one line and one plane.

The last case can be considered as a degeneration of the previous one, where the two points on the rims identify the contact line, while the point on the shoulder identifies

the contact plane. Furthermore, the contact on two points on both shoulders is only possible when the condition

$$\epsilon_a/D \leq \epsilon_r/L \tag{3.42}$$

where ϵ_a is the axial clearance, ϵ_r is the radial clearance, D is the shoulder diameter, and L is the pin length. The occurrence of contact in clearance-affected journal bearings is detailed in [8].

The maximization of function f is performed using the Lagrange multipliers technique; in order to use this technique, all three contacts have to be considered.

Contact on four points

Considering all four constraint functions (3.40) at the same time implies four contact points, two on the rims and two on the shoulder. The four inequalities become equations; the last two equations in (3.40) provide

$$\begin{aligned} \Delta z_i &= 0 \\ \theta_i &= 2\epsilon_a/D \end{aligned} \tag{3.43}$$

while the first two equations provide

$$\begin{aligned} \rho_i^2 &= \epsilon_r^2 - \epsilon_a^2 \tfrac{L^2}{D^2} \\ \psi_i &= \phi_i \pm \pi \end{aligned} \tag{3.44}$$

It clearly appears that the contact on four points is only possible if

$$\epsilon_r^2 - \epsilon_a^2 \frac{L^2}{D^2} \geq 0 \tag{3.45}$$

Moreover, it can be assumed

$$\psi_i = \phi_i \tag{3.46}$$

if both positive and negative value for ρ_i are accounted for. f becomes then function of ϕ_i only,

$$f = K_{i,1}\rho_i \cos(\phi_i) + K_{i,2}\rho_i \sin(\phi_i) + K_{i,4}\frac{2\epsilon_a}{D}\cos(\phi_i) + K_{i,5}\frac{2\epsilon_a}{D}\sin(\phi_i) \tag{3.47}$$

and reaches its maxima/minima when

$$\left(K_{i,1}\rho_i + K_{i,4}\frac{2\epsilon_a}{D}\right)\sin(\phi_i) = \left(K_{i,2}\rho_i + K_{i,5}\frac{2\epsilon_a}{D}\right)\cos(\phi_i) \tag{3.48}$$

Equation (3.48) provides four values for ϕ_i: two are obtained with $\rho_i = \sqrt{\epsilon_r^2 - \epsilon_a^2 \frac{L^2}{D^2}}$, and two with $\rho_i = -\sqrt{\epsilon_r^2 - \epsilon_a^2 \frac{L^2}{D^2}}$. The numerical value of f can be evaluated for each of the four solutions, so as to determine which solution generates the global maximum/minimum.

Contact on two points on the shoulder and one point on the rim

When three constraint functions from inequalities become equations, three contact points are imposed. If the third and the fourth of (3.40) are considered, two contact points lie on the two shoulders. The third contact point is on one of the rims: the upper one if the first constraint in (3.40) holds as an equation, the lower one if the second does. From hereon, the constraint set

$$\begin{cases} \rho_i^2 + \frac{L^2}{4}\theta_i^2 + \rho_i \theta_i L \sin(\psi_i - \phi_i) = \epsilon_r^2 \\ \rho_i^2 + \frac{L^2}{4}\theta_i^2 - \rho_i \theta_i L \sin(\psi_i - \phi_i) \leq \epsilon_r^2 \\ \frac{D}{2}\theta_i + \Delta z_i = \epsilon_a \\ \frac{D}{2}\theta_i - \Delta z_i = \epsilon_a \end{cases} \tag{3.49}$$

will be considered; however, all results are the same for the set

$$\begin{cases} \rho_i^2 + \frac{L^2}{4}\theta_i^2 + \rho_i \theta_i L \sin(\psi_i - \phi_i) \leq \epsilon_r^2 \\ \rho_i^2 + \frac{L^2}{4}\theta_i^2 - \rho_i \theta_i L \sin(\psi_i - \phi_i) = \epsilon_r^2 \\ \frac{D}{2}\theta_i + \Delta z_i = \epsilon_a \\ \frac{D}{2}\theta_i - \Delta z_i = \epsilon_a \end{cases} \tag{3.50}$$

The third and fourth equations in (3.49) yield

$$\begin{aligned} \Delta z_i &= 0 \\ \theta_i &= 2\epsilon_a / D \end{aligned} \tag{3.51}$$

The maximization problem can then be studied by using the Lagrange multipliers technique; the function

$$f = K_{i,1}\rho_i \cos(\phi_i) + K_{i,2}\rho_i \sin(\phi_i) + K_{i,4}\theta_i \cos(\psi_i) + K_{i,2}\theta_i \sin(\psi_i) \tag{3.52}$$

subject to the constraint

$$v = \rho_i^2 + \frac{L^2}{4}\theta_i^2 + \rho_i \theta_i L \sin(\psi_i - \phi_i) - \epsilon_r^2 = 0 \tag{3.53}$$

has to be maximized. An auxiliary function has to be introduced in order to apply the Lagrange multipliers technique. Such an auxiliary function can be defined as

$$F = f + \lambda v \tag{3.54}$$

where λ is a scalar parameter (multiplier). The local maxima/minima have then to satisfy the condition $\nabla F = 0$, leading to the non-linear system

$$\begin{cases} (K_{i,1}\cos(\phi_i) + K_{i,2}\sin(\phi_i)) + 2\lambda\rho_i + \lambda\theta_i L\sin(\psi_i - \phi_i) = 0 \\ \rho_i(-K_{i,1}\sin(\phi_i) + K_{i,2}\cos(\phi_i)) - \rho_i\lambda\theta_i L\cos(\psi_i - \phi_i) = 0 \\ \theta_i(-K_{i,4}\sin(\psi_i) + K_{i,5}\cos(\psi_i)) + \rho_i\lambda\theta_i L\cos(\psi_i - \phi_i) = 0 \\ \rho_i^2 + \frac{L^2}{4}\theta_i^2 + \rho_i\theta_i L\sin(\psi_i - \phi_i) - \epsilon_r^2 = 0 \end{cases} \tag{3.55}$$

in the unknown ρ_i, ϕ_i, ψ_i, and λ. The system can be re-arranged as

$$\begin{cases} \lambda\theta_i L\sin(\psi_i - \phi_i) = -(K_{i,1}\cos(\phi_i) + K_{i,2}\sin(\phi_i)) - 2\lambda\rho_i \\ \rho_i\lambda\theta_i L\cos(\psi_i - \phi_i) = \rho_i(-K_{i,1}\sin(\phi_i) + K_{i,2}\cos(\phi_i)) \\ \rho_i\lambda\theta_i L\cos(\psi_i - \phi_i) = -\theta_i(-K_{i,4}\sin(\psi_i) + K_{i,5}\cos(\psi_i)) \\ \rho_i\theta_i L\sin(\psi_i - \phi_i) = +\epsilon_r^2 - \rho_i^2 - \frac{L^2}{4}\theta_i^2 \end{cases} \tag{3.56}$$

The first and the fourth equations yield

$$-\rho_i(K_{i,1}\cos(\phi_i) + K_{i,2}\sin(\phi_i)) - 2\lambda\rho_i^2 = \lambda\left(\epsilon_r^2 - \rho_i^2 - \frac{L^2}{4}\theta_i^2\right) \tag{3.57}$$

while the combination of the first and second equation yields

$$\theta_i^2\lambda^2 L^2 - 4\rho_i^2\lambda^2 - \left(K_{i,1}^2 + K_{i,2}^2\right) = 4\rho_i\lambda(K_{i,1}\cos(\phi_i) + K_{2,i}\sin(\phi_i)) \tag{3.58}$$

By combining Eqs. (3.57) and (3.58),

$$\lambda^2 = \left(K_{i,1}^2 + K_{i,2}^2\right)/4\epsilon_r^2 \tag{3.59}$$

Equation (3.59) determines two possible values for λ. After λ has been determined, the system can be reduced to

$$A\rho_i^8 + B\rho_i^6 + C\rho_i^4 + D\rho_i^2 + E = 0 \tag{3.60}$$

where A, B, C, D, and E are numerical coefficients:

$$A = 64L^2(K_{i,1}^2 + K_{i,2}^2)^2$$

$$B = -32L(K_{i,1}^2 + K_{i,2}^2)\Big[L(K_{i,1}^2 + K_{i,2}^2)(4\epsilon_r^2 + L^2\theta_i^2) + \\ +2(K_{i,2}K_{i,4} - K_{i,5}K_{i,1})(4\epsilon_r^2 - \theta_i^2 L^2)\Big]$$

$$\begin{aligned} C = (4\epsilon_r^2 - \theta_i^2 - L^2)\Big[L^2(4\epsilon_r^2 - \theta_i^2 - L^2)(K_{i,1}^4 + K_{i,2}^4 + 2K_{i,1}^2 + 2K_{i,2}^2) \\ +8L(4\epsilon_r^2 + \theta_i^2 L^2)(K_{i,1}^2 + K_{i,2}^2)(K_{i,4}K_{i,2} - K_{i,1}K_{i,5})\Big] + \\ +\theta_i^2 L^2 \epsilon_r^2 \Big[128K_{i,1}K_{i,2}K_{i,4}K_{i,5} + 4(16\epsilon_r^4 + \theta_i^4 L^4)(K_{i,4}^2 + K_{i,5}^2)(K_{i,1}^2 + K_{i,2}^2) \\ +32(K_{i,5}^2 - K_{i,4}^2)(K_{i,2}^2 - K_{i,1}^2)\Big] \end{aligned} \tag{3.61}$$

$$D = -4(K_{i,1}^2 + K_{i,1}^2)(L\theta_i - 2\epsilon)^2(L\theta_i + 2\epsilon)^2 \\ \Big[L(k_{i,5}K_{i,1} - K_{i,4}K_{i,2})(L^2\theta_i^2 - 4\epsilon^2) + 2(K_{i,4}^2 + K_{i,5}^2)(L^2\theta_i^2 + 4\epsilon^2)\Big]$$

$$E = (K_{i,4}^2 + K_{i,5}^2)(K_{i,2}^2 + K_{i,1}^2)(L\theta_i - 2\epsilon)^4(L\theta_i + 2\epsilon)^4$$

Equation (3.60) provides up 8 solutions for ρ_i. For each pair $\{\lambda_i, \pm\rho_i\}$ it is possible to find two values for ϕ_i (Eq. (3.57)); for each ϕ_i, two values of ψ_i (third equation in (3.55)). In this way, up to 64 solution sets can be identified for the non-linear system (3.57). Among these sets, those which do not satisfy the inequality in (3.49) have to be discarded. Each of the remaining sets can generate a local maximum/minimum. The evaluation of function (3.52) with all solution sets, and the comparison of the consequent values, allow the determination of the global maximum/minimum.

Contact on two points on the rim and one point on the shoulder

When three constraint functions from inequalities become equations, three contact points are imposed. If the first and the second inequalities in (3.40) are considered, two contact points lie on the rim. The third contact point is on one of the shoulder: the upper one if the fourth constraint in (3.40) holds as an equation, the lower one

if the third does. From here on, the constraint set

$$\begin{cases} \rho_i^2 + \frac{L^2}{4}\theta_i^2 + \rho_i\theta_i L\sin(\psi_i - \phi_i) = \epsilon_r^2 \\ \rho_i^2 + \frac{L^2}{4}\theta_i^2 - \rho_i\theta_i L\sin(\psi_i - \phi_i) = \epsilon_r^2 \\ \frac{D}{2}\theta_i + \Delta z_i = \epsilon_a \\ \frac{D}{2}\theta_i - \Delta z_i \leq \epsilon_a \end{cases} \tag{3.62}$$

will be considered; however, all results are the same for the set

$$\begin{cases} \rho_i^2 + \frac{L^2}{4}\theta_i^2 + \rho_i\theta_i L\sin(\psi_i - \phi_i) = \epsilon_r^2 \\ \rho_i^2 + \frac{L^2}{4}\theta_i^2 - \rho_i\theta_i L\sin(\psi_i - \phi_i) = \epsilon_r^2 \\ \frac{D}{2}\theta_i + \Delta z_i \leq \epsilon_a \\ \frac{D}{2}\theta_i - \Delta z_i = \epsilon_a \end{cases} \tag{3.63}$$

The first and second equations in (3.62) yield

$$\begin{aligned} \psi_i &= \phi_i \pm \pi \\ \rho_i^2 + \tfrac{L^2}{4}\theta_i^2 &= \epsilon_r \end{aligned} \tag{3.64}$$

The first condition in (3.64) expresses the fact that the translation in a plane orthogonal to the pair axis $[\rho_i\cos(\phi_i), \rho_i\sin(\phi_i)]$ occurs along the rotation axis identified by θ_i, and can have both directions. If both positive and negative values are considered for ρ_i, the condition can be simplified to

$$\psi_i = \phi_i \tag{3.65}$$

The maximization problem can then be studied by using the Lagrange multipliers technique; the function

$$f = K_{i,1}\rho_i\cos(\phi_i) + K_{i,2}\rho_i\sin(\phi_i) + K_{i,3}\Delta z_i + K_{i,4}\theta_i\cos(\phi_i) + K_{i,2}\theta_i\sin(\phi_i) \tag{3.66}$$

subject to the constraints

$$\begin{aligned} v_1 &= \rho_i^2 + \tfrac{L^2}{4}\theta_i^2 - \epsilon_r^2 = 0 \\ v_2 &= \tfrac{D}{2}\theta_i + \Delta z_i - \epsilon_a = 0 \end{aligned} \tag{3.67}$$

has to be maximized. An auxiliary function has to be introduced in order to apply the Lagrange multipliers technique. Such an auxiliary function is

$$F = f + \lambda v_1 + \mu v_2 \tag{3.68}$$

where λ and μ are scalar parameters. The local maxima/minima have then to satisfy the condition $\nabla F = 0$, leading to the non-linear system

$$\begin{cases} (K_{i,1}\cos(\phi_i) + K_{i,2}\sin(\phi_i)) + 2\lambda\rho_i = 0 \\ \rho_i(-K_{i,1}\sin(\phi_i) + K_{i,2}\cos(\phi_i)) + \theta_i(-K_{i,4}\sin(\phi_i) + K_{i,5}\cos(\phi_i)) = 0 \\ (K_{i,4}\cos(\phi_i) + K_{i,5}\sin(\phi_i)) + \frac{L^2}{2}\lambda\theta_i + \frac{D}{2}\mu = 0 \\ K_{i,3} + \mu = 0 \\ \rho_i^2 + \frac{L^2}{4}\theta_i^2 - \epsilon_r^2 = 0 \\ \frac{D}{2}\theta_i + \Delta z_i - \epsilon_a = 0 \end{cases} \tag{3.69}$$

in the unknown ρ_i, θ_i, ϕ_i, Δz_i, λ, and μ. From the fourth equation,

$$\mu = -K_{i,3} \tag{3.70}$$

while, from the first two,

$$\begin{aligned} \cos(\phi_i) &= -2\lambda\rho_i \frac{K_{i,1}\rho_i + K_{i,4}\theta_i}{\rho_i\left(K_{i,1}^2 + K_{i,2}^2\right) + \theta_i\left(K_{i,4}K_{i,1} + K_{i,2}K_{i,5}\right)} \\ \sin(\phi_i) &= -2\lambda_i\rho_i \frac{K_{i,2}\rho_i + K_{i,5}\theta_i}{\rho_i\left(K_{i,1}^2 + K_{i,2}^2\right) + \theta_i\left(K_{i,4}K_{i,1} + K_{i,2}K_{i,5}\right)} \end{aligned} \tag{3.71}$$

It is then possible to obtain λ from the third equation,

$$\lambda = \mu D \frac{\rho_i\left(K_{i,1}^2 + K_{i,2}^2\right) + \theta_i\left(K_{i,1}K_{i,4} + K_{i,2}K_{i,5}\right)}{\left(K_{i,1}K_{i,4} + K_{i,2}K_{i,5}\right)\left(4\rho_i^2 + L^2\theta_i^2\right) - \rho_i\theta_i\left[L\left(K_{i,1}^2 + K_{i,2}^2\right) - 4\left(K_{i,4}^2 + K_{i,5}^2\right)\right]} \tag{3.72}$$

Equations (3.71) can then be combined; the result is

$$A\rho_i^4 + B\rho_i^3\theta_i + C\rho_i^2\theta_i^2 + D\rho_i\theta_i^3 + E\theta_i^4 = 0 \tag{3.73}$$

where A, B, C, D, and E are numerical coefficients:

$$\begin{aligned} A &= 4\mu^2D^2\left(K_{i,1}^2 + K_{i,2}^2\right) - 16\left(K_{i,1}K_{i,4} + K_{i,2}K_{i,5}\right)^2 \\ B &= 8\left(K_{i,1}K_{i,4} + K_{i,2}K_{i,5}\right) + \left[L^2\left(K_{i,1}^2 + K_{i,2}^2\right) - 4\left(K_{i,4}^2 + K_{i,5}^2\right) + \mu^2D^2\right] \\ C &= 4\mu^2D^2\left(K_{i,4}^2 + K_{i,5}^2\right) - 16\left(K_{i,4}^2 + K_{i,5}^2\right)^2 - L^4\left(K_{i,1}^2 + K_{i,2}^2\right)^2 + \\ &\quad + 8L^2\left(K_{i,1}K_{i,5} + K_{i,2}K_{i,4}\right)^2 + 16L^2\left(K_{i,1}^2K_{i,4}^2 + K_{i,2}^2K_{i,5}^2\right) \\ D &= -2L^2\left(K_{i,1}K_{i,4} + K_{i,2}K_{i,5}\right)\left[L^2\left(K_{i,1}^2 + K_{i,2}^2\right) - 4\left(K_{i,4}^2 + K_{i,5}^2\right)\right] \\ E &= -L^4\left(K_{i,1}K_{i,4} + K_{i,2}K_{i,5}\right)^2 \end{aligned} \tag{3.74}$$

Considering the fifth equation in (3.69), Eq. (3.73) can be reduced to a 8th-degree biquadratic equation, in the form

$$A'\rho_i^8 + B'\rho_i^6 + C'\rho_i^4 + D'\rho_i^2 + E' = 0 \tag{3.75}$$

with

$$\begin{aligned} A' &= \epsilon_r^8 \left[(2L)^2 \left(L^2 B - 4D \right)^2 + \left(AL^4 + 4CL^2 + 16E \right)^2 \right] \\ B' &= 4\epsilon_r^3 \left[2 \left(CL^2 - 8E \right) \left(AL^4 - 4CL^2 + 16E \right) - L^2 \left(12D - L^2 B \right) \left(4D - L^2 B \right) \right] \\ C' &= 16\epsilon_r^2 \left[CL^2 \left(CL^2 - 24E \right) + 2E \left(AL^4 + 48E^2 \right) + 2L^2 D \left(6D - L^2 B \right) \right] \\ D' &= -64\epsilon_r^2 \left[E^2 + L^2 \left(D^2 - 2EC \right) \right] \\ E' &= 256E^2 \end{aligned} \tag{3.76}$$

Up to 8 real solutions exist for Eq. (3.75). They can be found in a closed form. For each value of ρ_i, up to 4 values for θ_i can be found through Eq. (3.73). Once a set $\{\rho_i, \theta_i\}$ has been determined, Eqs. (3.72) and (3.71) determine one value for λ and ϕ. The last equation in (3.69) provides one value for Δz_i. In this way, up to 32 solutions can be found for the non linear system (3.69). Each set can generate a local maximum/minimum. The evaluation of function (3.66) with all solution sets, and the comparison of the consequent values, allow the determination of the global maximum/minimum.

After the local maxima/minima have been determined for each kind of contact, the comparison between their numerical value permits determining

- the global maximum/minimum;
- the kind of contact associated with it;
- the values of the contact parameters ρ_i, θ_i, ϕ_i, ψ_i, and Δz_i generating it.

3.3.2 Cylindrical Pair

The sub-function concerning a cylindrical pair has the form

$$f = K_{j,1}\rho_j \cos(\phi_j) + K_{j,2}\rho_j \sin(\phi_j) + K_{j,4}\theta_j \cos(\psi_j) + K_{j,5}\theta_j \sin(\psi_j) \tag{3.77}$$

subject to the constraints

$$\begin{cases} \rho_j^2 + \frac{L^2}{4}\theta_j^2 + \rho_j\theta_j L\sin(\psi_j - \phi_j) \leq \epsilon_r^2 \\ \rho_j^2 + \frac{L^2}{4}\theta_j^2 - \rho_i\theta_j L\sin(\psi_j - \phi_j) \leq \epsilon_r^2 \end{cases} \tag{3.78}$$

When the maximum for f is to be looked for on the domain border; inside the domain, local maxima have to satisfy the condition $\nabla f{=}0$, which leads to the system

$$\begin{cases} K_{j,1}\cos(\phi_j) + K_{j,2}\sin(\phi_j) = 0 \\ -K_{j,1}\rho_j\sin(\phi_j) + K_{i,2}\rho_j\cos(\phi_j) = 0 \\ K_{j,4}\cos(\psi_j) + K_{j,5}\sin(\psi_j) = 0 \\ -K_{j,4}\theta_j\sin(\phi_j) + K_{j,5}\theta_j\sin(\psi_i) = 0 \end{cases} \tag{3.79}$$

whose only solution gives a null value for both ρ_i and θ_i; such a solution is neither the function minimum nor its maximum. The domain border is defined by the constraints (3.78), which can be combined to obtain

$$\begin{gathered} \rho_j^2 + \frac{L^2}{4}\theta_j^2 - \epsilon^2 \\ \psi_j = \phi_j \pm \pi \end{gathered} \tag{3.80}$$

As for the revolute pair, when positive and negative values are considered for ρ_j, it is possible to assume

$$\psi_j = \phi_j \tag{3.81}$$

The maximization of function f is performed using the Lagrange multipliers technique. An auxiliary function has to be introduced in order to apply the technique. Such an auxiliary function can be defined as

$$F = f + \lambda\left(\rho_j^2 + \frac{L^2}{4}\theta_j^2 - \epsilon^2\right) \tag{3.82}$$

where λ is a scalar parameter (multiplier). The local maxima/minima have to satisfy the condition $\nabla F = 0$, leading to the non-linear system

$$\begin{cases} (K_{j,1}\cos(\phi_j) + K_{j,2}\sin(\phi_j)) + 2\lambda\rho_j = 0 \\ \rho_j(-K_{j,1}\sin(\phi_j) + K_{j,2}\cos(\phi_j)) + \theta_j(-K_{j,4}\sin(\phi_j) + K_{j,5}\cos(\phi_j)) = 0 \\ (K_{j,4}\cos(\phi_j) + K_{j,5}\sin(\phi_j)) + \frac{L^2}{2}\lambda\theta_j = 0 \\ \rho_j^2 + \frac{L^2}{4}\theta_j^2 - \epsilon^2 \end{cases} \tag{3.83}$$

in the unknown ρ_i, ϕ_i, and λ. The non linear system (3.83) can be solved like (3.69). Up to 32 solution sets exist, which means that there are up to 32 local

maxima/minima. The evaluation of function (3.77) with all solution sets, and the comparison of the consequent values, allow the determination of the global maximum/minimum.

3.3.3 Spherical Pair

The sub-function concerning a spherical pair has the form

$$f = K_{k,1}\rho_k \cos(\phi_k)\cos(\psi_k) + K_{k,2}\rho_k \cos(\phi_k)\sin(\psi_k) + K_{k,3}\rho_k \sin(\psi_k) \tag{3.84}$$

subject to the constraint

$$v = 0 \leq \rho_k \leq \epsilon \tag{3.85}$$

The maximum for f is to be looked for on the domain border; inside the domain, local maxima have to satisfy the condition ∇f=0, which leads to the system

$$\begin{cases} K_{j,1}\cos(\phi_j) + K_{j,2}\sin(\phi_j) = 0 \\ -K_{j,1}\rho_j \sin(\phi_j) + K_{i,2}\rho_j \cos(\phi_j) = 0 \\ K_{j,4}\cos(\psi_j) + K_{j,5}\sin(\psi_j) = 0 \\ -K_{j,4}\theta_j \sin(\phi_j) + K_{j,5}\theta_j \sin(\psi_i) = 0 \end{cases} \tag{3.86}$$

whose only solution gives a null value for ρ_j (provided that at least one among $K_{k,1}$, $K_{k,2}$, and $K_{k,3}$ is not null); such a solution is neither a minimum nor a maximum. The domain border is defined by

$$\rho_k = \epsilon \tag{3.87}$$

Function f becomes then

$$f = K_{k,1}\epsilon \cos(\phi_k)\cos(\psi_k) + K_{k,2}\epsilon \cos(\phi_k)\sin(\psi_k) + K_{k,3}\epsilon \sin(\psi_k) \tag{3.88}$$

and its maxima/minima have to satisfy the condition $\nabla f = 0$, leading to the non linear system

$$\begin{cases} \epsilon\cos(\phi_k)\left(-K_{k,1}\cos(\phi_k) + K_{k,2}\sin(\phi_k)\right) = 0 \\ \epsilon\sin(\psi_k)\left(-K_{k,1}\cos(\phi_k) + K_{k,2}\sin(\phi_k)\right) + \epsilon K_{k,3}\cos(\psi_k) = 0 \end{cases} \tag{3.89}$$

in the unknowns ϕ_k and ψ_k only. Up to eight solutions can be easily found for such a system. The evaluation of function (3.84) for all solution sets, and the comparison of the consequent values, allow the determination of the global maximum/minimum.

3.3.4 Prismatic Pair

The sub-function concerning a prismatic pair has the form

$$f = K_{l,1}\Delta x_l + K_{l,2}\Delta y_l + K_{l,4}\Delta\xi_l + K_{l,5}\Delta\eta_l + K_{l,6}\Delta\zeta_l \tag{3.90}$$

subject to the constraints

$$\begin{cases} -l\Delta\eta_l - 2\Delta x_l - a\Delta\zeta_l \le 2\epsilon & -l\Delta\xi_l - 2\Delta y_l - a\Delta\zeta_l \le 2\epsilon \\ -l\Delta\eta_l - 2\Delta x_l + a\Delta\zeta_l \le 2\epsilon & -l\Delta\xi_l - 2\Delta y_l + a\Delta\zeta_l \le 2\epsilon \\ -l\Delta\eta_l + 2\Delta x_l - a\Delta\zeta_l \le 2\epsilon & -l\Delta\xi_l + 2\Delta y_l - a\Delta\zeta_l \le 2\epsilon \\ -l\Delta\eta_l + 2\Delta x_l + a\Delta\zeta_l \le 2\epsilon & -l\Delta\xi_l + 2\Delta y_l + a\Delta\zeta_l \le 2\epsilon \\ l\Delta\eta_l - 2\Delta x_l - a\Delta\zeta_l \le 2\epsilon & l\Delta\xi_l - 2\Delta y_l - a\Delta\zeta_l \le 2\epsilon \\ l\Delta\eta_l - 2\Delta x_l + a\Delta\zeta_l \le 2\epsilon & l\Delta\xi_l - 2\Delta y_l + a\Delta\zeta_l \le 2\epsilon \\ l\Delta\eta_l + 2\Delta x_l - a\Delta\zeta_l \le 2\epsilon & l\Delta\xi_l + 2\Delta y_l - a\Delta\zeta_l \le 2\epsilon \\ l\Delta\eta_l + 2\Delta x_l + a\Delta\zeta_l \le 2\epsilon & l\Delta\xi_l + 2\Delta y_l + a\Delta\zeta_l \le 2\epsilon \end{cases} \tag{3.91}$$

Since f is a linear function, its maximum is to be found on the domain border. The domain is defined by the inequalities (3.91); its border can be obtained by changing all inequalities into equations. The shape of the domain defined by (3.91) is not easy to figure out, as it involves five variables - Δx_l, Δy_l, $\Delta\xi_l$, $\Delta\eta_l$, and $\Delta\zeta_l$ - and therefore a 5-dimensional space. In order to better understand it, it can be noted that the variables are almost completely decoupled, in the sense that no equation contains Δx_l and Δy_l at the same time, or $\Delta\xi_l$ and $\Delta\eta_l$. $\Delta\zeta_l$ only appears in all equations. The system (3.91) can then be split in two parts,

$$\begin{cases} -l\Delta\eta_l - 2\Delta x_l - a\Delta\zeta_l = 2\epsilon & -l\Delta\eta_l - 2\Delta x_l + a\Delta\zeta_l = 2\epsilon \\ -l\Delta\eta_l + 2\Delta x_l - a\Delta\zeta_l = 2\epsilon & -l\Delta\eta_l + 2\Delta x_l + a\Delta\zeta_l = 2\epsilon \\ l\Delta\eta_l - 2\Delta x_l - a\Delta\zeta_l = 2\epsilon & l\Delta\eta_l - 2\Delta x_l + a\Delta\zeta_l = 2\epsilon \\ l\Delta\eta_l + 2\Delta x_l - a\Delta\zeta_l = 2\epsilon & l\Delta\eta_l + 2\Delta x_l + a\Delta\zeta_l = 2\epsilon \end{cases} \tag{3.92}$$

and

$$\begin{cases} -l\Delta\xi_l - 2\Delta y_l - a\Delta\zeta_l = 2\epsilon & -l\Delta\xi_l - 2\Delta y_l + a\Delta\zeta_l = 2\epsilon \\ -l\Delta\xi_l + 2\Delta y_l - a\Delta\zeta_l = 2\epsilon & -l\Delta\xi_l + 2\Delta y_l + a\Delta\zeta_l = 2\epsilon \\ l\Delta\xi_l - 2\Delta y_l - a\Delta\zeta_l = 2\epsilon & l\Delta\xi_l - 2\Delta y_l + a\Delta\zeta_l = 2\epsilon \\ l\Delta\xi_l + 2\Delta y_l - a\Delta\zeta_l = 2\epsilon & l\Delta\xi_l + 2\Delta y_l + a\Delta\zeta_l = 2\epsilon \end{cases} \tag{3.93}$$

The system (3.92) defines eight planes in the 3-dimensional space $\{\Delta x_l, \Delta\eta_l, \Delta\zeta_l\}$. The eight planes define a diamond-shaped volume, shown in Fig. 3.5. On the other

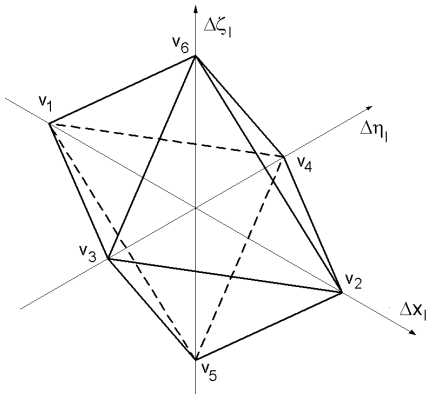

Figure 3.5: Domain for $\{\Delta x_l, \Delta\eta_l, \Delta\zeta_l\}$

hand, the part of function f involving the three variables Δx_l, $\Delta\eta_l$, and $\Delta\zeta_l$ is

$$f^1 = K_{l,1}\Delta x_l + K_{l,4}\Delta\eta_l + K_{l,5}\Delta\zeta_l \tag{3.94}$$

and defines a plane in the same space. Consequently, the maximum of f^1 has to be on one of the vertices v_n, n=1..6, defined in Table 3.1.

Similarly, it is possible to define a 3-dimensional space $\{\Delta y_l, \Delta\xi_l, \Delta\zeta_l\}$, and a function f^2 as

$$f^2 = K_{l,2}\Delta y_l + K_{l,3}\Delta\xi_l + K_{l,5}\Delta\zeta_l \tag{3.95}$$

The sistem (3.93) defines a diamond-shaped volume similar to that in Fig. 3.5, whose vertices u_n, n=1..6, are reported in Table 3.2. The maximum of f^2 has to be in one of those vertices.

Even if the two spaces $\{\Delta x_l, \Delta\eta_l, \Delta\zeta_l\}$ and $\{\Delta y_l, \Delta\xi_l, \Delta\zeta_l\}$ have one variable in common, vertices v_n and u_n are completely independent. As a consequence, when f^1 and f^2 are maximized/minimized at the same time, the union of the two sets v_n and u_n has to be considered: the global maximum/minimum for function f has to be in one of the points reported in Table 3.3. The evaluation of function (3.90) for all points in Table 3.3, and the comparison of the consequent values, allows determining its global maximum/minimum.

3.4 Numerical Example

A parallel manipulator with three dofs, known as Tsai Manipulator [30], is studied. The mechanism shown in Fig. 3.6. It consists of two platforms, one assumed as

Table 3.1: Domain vertices for Δx_l, $\Delta \eta_l$, and $\Delta \zeta_l$

Vertex	Δx_l	$\Delta \eta_l$	$\Delta \zeta_l$
v_1	$-\epsilon$	0	0
v_2	$+\epsilon$	0	0
v_3	0	$-2\epsilon/l$	0
v_4	0	$+2\epsilon/l$	0
v_5	0	0	$-2\epsilon/a$
v_6	0	0	$+2\epsilon/a$

Table 3.2: Domain vertices for Δy_l, $\Delta \xi_l$, and $\Delta \zeta_l$

Vertex	Δx_l	$\Delta \eta_l$	$\Delta \zeta_l$
u_1	$-\epsilon$	0	0
u_2	$+\epsilon$	0	0
u_3	0	$-2\epsilon/l$	0
u_4	0	$+2\epsilon/l$	0
u_5	0	0	$-2\epsilon/a$
u_6	0	0	$+2\epsilon/a$

Table 3.3: Domain vertices for Δx_l, Δy_l, Δxi_l, $\Delta \eta_l$, and $\Delta \zeta_l$

Vertex	Δx_l	Δy_l	$\Delta \xi_l$	$\Delta \eta_l$	$\Delta \zeta_l$
1	$-\epsilon$	0	$-\epsilon$	0	0
2	$-\epsilon$	0	$+\epsilon$	0	0
3	$-\epsilon$	0	0	-2ϵ/l	0
4	$-\epsilon$	0	0	$+2\epsilon/l$	0
5	$+\epsilon$	0	$-\epsilon$	0	0
6	$+\epsilon$	0	$+\epsilon$	0	0
7	$+\epsilon$	0	0	-2ϵ/l	0
8	$+\epsilon$	0	0	$+2\epsilon/l$	0
9	0	-2ϵ/l	$-\epsilon$	0	0
10	0	-2ϵ/l	$+\epsilon$	0	0
11	0	-2ϵ/l	0	-2ϵ/l	0
12	0	-2ϵ/l	0	$+2\epsilon/l$	0
13	0	$+2\epsilon/l$	$-\epsilon$	0	0
14	0	$+2\epsilon/l$	$+\epsilon$	0	0
15	0	$+2\epsilon/l$	0	-2ϵ/l	0
16	0	$+2\epsilon/l$	0	$+2\epsilon/l$	0
17	0	0	0	0	-2ϵ/a
18	0	0	0	0	$+2\epsilon/a$

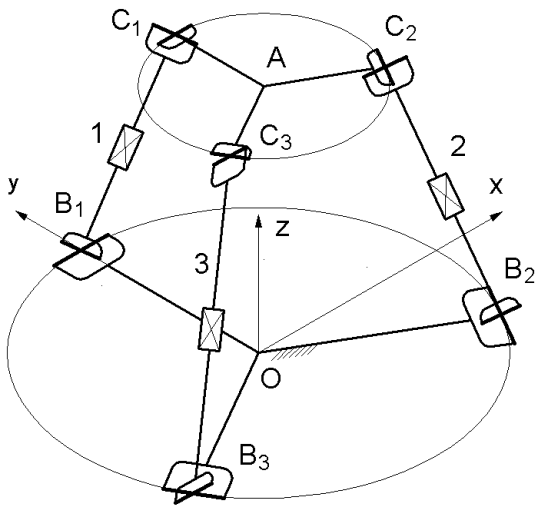

Figure 3.6: Tsai Manipulator

the frame (base) and the other one as end-effector (platform). The two platforms are connected by three serial kinematic chains (legs), each one composed of a first passive universal joint, a controlled prismatic pair and a second passive universal joint. Under some geometric and mounting conditions, the platform has a pure translational motion [30]. The universal joint centers on both the base and the platform are located at the vertices of two equilateral triangles, inscribed in two circles with radius 200 and 100 respectively (all lengths are in arbitrary length units). The three revolute pair axes on the base and on the platform form equilateral triangles. Each universal joint is modelled as the union of two clearance-affected revolute pairs, whose dimension (with reference to Fig. 3.1) are $D = 2$, $L = 5$, $\varepsilon_r = 0.01$, $\varepsilon_a = 0.01$.

The mechanism is controlled by the length of the three legs, and provides the platform position as output. The platform position can be represented by the position of its geometrical center, point A in Fig. 3.6, in an absolute reference system. A reference system centered in the base geometrical center, with the z-axis orthogonal to the base and the y-axis passing through the center of one universal joint has been chosen as the absolute one. The aim of the analysis is to find the displacement of the platform due to clearance in the revolute pairs. In order to apply the method the mechanism configuration has to be assigned. The configuration defined by $A = [87, -37, 85]$ has been chosen.

The kinematic analysis previously described can be used to define the pose error function. For the sake of clarity, only the third component of the pose error function - the position error in the vertical direction - is reported.

$$\Delta\Gamma_3 = \begin{bmatrix} +0.16439 \cdot \rho_{11} \sin\phi_{11} + 0.088706 \cdot \Delta z_{11} - 75.866 \cdot \theta_{11} \sin\psi_{11} \\ +0.16439 \cdot \rho_{12} \cos\phi_{12} + 0.088706 \cdot \rho_{12} \sin\phi_{12} - 75.866 \cdot \theta_{12} \cos\psi_{12} \\ +0.16439 \cdot \rho_{13} \cos\phi_{13} + 0.088706 \cdot \rho_{13} \sin\phi_{13} - 75.866 \cdot \theta_{13} \cos\psi_{13} \\ +0.16439 \cdot \rho_{14} \sin\phi_{14} + 0.088706 \cdot \Delta z_{14} - 75.866 \cdot \theta_{14} \sin\psi_{14} \\ +0.96127 \cdot \rho_{21} \sin\phi_{21} - 0.12925 \cdot \Delta z_{21} + 16.246 \cdot \theta_{21} \sin\psi_{21} \\ +0.96127 \cdot \rho_{22} \cos\phi_{22} - 0.12925 \cdot \rho_{22} \sin\phi_{22} + 16.246 \cdot \theta_{22} \cos\psi_{22} \\ +0.96127 \cdot \rho_{23} \cos\phi_{23} - 0.12925 \cdot \rho_{23} \sin\phi_{23} + 16.246 \cdot \theta_{23} \cos\psi_{23} \\ +0.96127 \cdot \rho_{24} \sin\phi_{24} - 0.12925 \cdot \Delta z_{24} + 16.246 \cdot \theta_{24} \sin\psi_{24} \\ -0.095720 \cdot \rho_{31} \sin\phi_{31} + 0.040537 \cdot \Delta z_{31} + 49.930 \cdot \theta_{31} \sin\psi_{31} \\ -0.095720 \cdot \rho_{32} \cos\phi_{32} + 0.040537 \cdot \rho_{32} \sin\phi_{32} + 49.930 \cdot \theta_{32} \cos\psi_{32} \\ -0.095720 \cdot \rho_{33} \cos\phi_{33} + 0.040537 \cdot \rho_{33} \sin\phi_{33} + 49.930 \cdot \theta_{33} \cos\psi_{33} \\ -0.095720 \cdot \rho_{34} \sin\phi_{34} + 0.040537 \cdot \Delta z_{34} + 49.930 \cdot \theta_{34} \sin\psi_{34} \end{bmatrix} \tag{3.96}$$

In Eq. (3.96), ρ_{ij}, θ_{ij}, ϕ_{ij}, ψ_{ij}, and Δz_{ij}, $i = 1..3$, $j = 1..4$, are the parameters referring to the j-th pair of the i-th leg. The pairs in each leg are numbered starting form the base, while the legs are numbered as shown in Fig. 3.6. These parameters are expressed in local reference systems. For each leg, the local reference systems are defined as follows:

- for the first pair (i.e., the pair fixed to the base), the local x-axis lies on the axis of the second revolute pair, the local z-axis is along the pair axis, and the y-axis is orthogonal to both according to the right-hand rule;
- for the second pair (i.e., the mobile pair in the base universal joint), the local y-axis lies on the axis of the first revolute pair, the local z-axis is along the pair axis, and the x-axis is orthogonal to both according to the right-hand rule;
- for the third pair, the local y-axis lies on the axis of the fourth revolute pair, the local z-axis is along the pair axis, and the x-axis is orthogonal to both according to the right-hand rule;
- for the fourth pair (i.e., the pair fixed to the platform), the local x-axis lies on

Table 3.4: Contact parameters for each pair

Leg	Pair	ρ	ϕ	Δz	θ	ψ	Contrib.
1	1	0.00005	$-\pi/2$	0.00600	0.0039999	$-\pi/2$	0.30399
1	2	-0.00005	-3.14157	0.00600	0.0039999	-3.14157	0.30346
1	3	-0.00005	-3.14157	0.00600	0.0039999	π	0.30346
1	4	0.00005	$-\pi/2$	0.00600	0.0039999	$-\pi/2$	0.30399
2	1	0.00147	$\pi/2$	-0.00604	0.0039563	$\pi/2$	0.06648
2	2	0.00146	-0.0028802	0.00604	0.0039569	-0.00288	0.06570
2	3	0.00146	-0.0028802	0.00604	0.0039569	-0.00288	0.06570
2	4	0.00147	$\pi/2$	-0.00604	0.0039563	$\pi/2$	0.06648
3	1	-0.00005	$\pi/2$	0.00600	0.0039999	$\pi/2$	0.19996
3	2	-0.00005	0.00001	0.00600	0.0039999	0.00001	0.19972
3	3	-0.00005	0.00001	0.00600	0.0039999	0.00001	0.19972
3	4	-0.00005	$\pi/2$	0.00600	0.0039999	$\pi/2$	0.19996

the axis of the third revolute pair, the local z-axis is along the pair axis, and the y-axis is orthogonal to both according to the right-hand rule.

The maximization of $\Delta\Gamma_3$ provides as result

$$\max(\Delta\Gamma_3) = 2.2786 \; l.u. \tag{3.97}$$

The maximizing values of the contact parameters and their contribution for each pair are reported in Table 3.4.

Conclusions

In this doctoral dissertation, a new method to asses the influence of clearance in the kinematic pairs on the configuration of planar and spatial mechanisms has been presented. Unlike previous methods, the approach to the clearance-problem is purely kinematic, as no knowledge of the loads acting on the mechanisms is needed to perform the analysis. Despite this, the displacements caused by clearance are modelled in a completely deterministic way.

With reference to a given mechanism configuration, the pose error of the mechanism link of interest is expressed as a vector function. Such a function involves the displacements in the clearance-affected pairs, considered as independent variables. These displacements are constrained by the geometry of the pair. The most common kinematic pairs (revolute, prismatic, cylindrical, and spherical) have been modelled, so that all constraints could be expressed by analytical functions. The problem has then be studied like a maximization problem, where a continuous function (the pose error of the link of interest) subject to some constraints (the analytical functions bounding clearance-due degrees of freedom) has to be maximize. The solution to the maximization problem has been obtained in a closed form for mechanisms containing revolute, prismatic, cylindrical, and/or spherical clearance-affected pairs.

Bibliography

[1] S. Dubowsky, J. Maatuk, and N.D Perreira, 1974, "A Parameter Identification Study of Kinematic Errors in Planar Mechanisms", *Journal of Engineering for Industry*, Vol. 97B, No. 2, pp. 635 - 642.

[2] Z.W. Yin, and J.K. Wu, 1990, "An Optimal Synthesis of Linkages considering Structural Error and Clearances", *Proceedings of 1990 ASME Mechanisms Conference*, Chicago, USA, pp. 295 - 299.

[3] A. Biswas, and G.L. Kinzel, "An Iterative Kinematic and Force Solution Method for Revolute Joints with Clearance", *Proceeding of 1998 ASME Design Engineering Technical Conference*, Atlanta, USA, Paper MECH-5491.

[4] P. Voglewede, and I. Ebert-Uphoff, 2002, "Application of Workspace Generation Techniques to Determine the Unconstrained Motion of Parallel Manipulators", *submitted to ASME Journal of Mechanical Design.*

[5] H. Hahn, 1994, "Mathematical Modelling and Computer Simulation of Rigid Body Systems including Spatial Joints with Clearance", *Proceedings of the 1st Joint Conference of International Simulation Societies*, Zurich, Switzerland, pp. 261 - 267.

[6] J. Phillips, 1971, "Geometry of Backlash in Spatial Mechanisms", *Proceedings of the 3rd World Congress on the Theory of Mechanisms and Machines*, Kupari, Jugoslavia.

[7] M. Horie, H. Funabashi, K. Ogawa, and H. Kobayashi, 1985, "A Displacement Analysis of Spatial Four-Bar Mechanisms", *Bulletin of JSME*, vol. 28, No. 241, pp. 1535 - 1542.

[8] H.S. Wang, and B. Roth, 1989, "Position Errors Due to Clearance in Journal Bearings", *Journal of Mechanisms, Transmissions, and Automation in Design*, vol. 111, pp. 315 - 320.

[9] C. Innocenti, 1999, "Kinematic Clearance Sensitivity Analysis of Spatial Structures with Revolute Joints", *Proceedings of the 1999 ASME Design Engineering Technical Conference*, Las Vegas, USA, Paper DAC-8679.

[10] V. Parenti-Castelli, and S. Venanzi, 2001, "Kinetostatic Behavior of the Prismatic Pair with Clearance", *Proceedings of the 2001 International Mechanical Engineering Congress and Exposition*, New York, USA.

[11] Z. Huang, 1987, "Error Analysis of Position and Orientation in Robot Manipulators", *Mechanism and Machine Theory*, Vol. 22, No. 6, pp. 577 - 581.

[12] H.H.S. Wang, and B. Roth, 1988, "Position Errors of Manipulators", *Proceedings of RoManSy 7*, Udine, Italia.

[13] W. Xu, and Q. Zhang, 1987, "On the Method of Combining Small Displacements in Studying the Kinematic Errors of Spatial Open- and Closed-Loop Linkages", *Proceedings of the 7th World Congress on the Theory of Machines and Mechanisms*, Sevilla, Spain, pp. 219 - 222.

[14] C.R. Tischler, and A.E. Samuel, 1998, "Predicting the Slop of In-Series/Parallel Manipulators Caused by Joint Clearances", *Advances in Robot Kinematics and Control*, Eds. J. Lenarcic and M.L. Husty, Kluwer Academic Publishers, pp. 227 - 236.

[15] V. Parenti-Castelli, S. Venanzi, and J. Lenarcic, 2001, "Influence of Geometry on the Kinematic Performances of a Humanoid Shoulder-Girdle Mechanism", *Proceedings of the 2001 IEEE/ASME International Conference on Advanced Intelligent Mechatronics*, Como, Italia.

[16] V. Parenti-Castelli, and S. Venanzi, 2002, "A New Deterministic Method for Clearance Influence Analysis in Spatial Mechanisms", *2002 ASME International Mechanical Engineering Congress and Exposition*, New Orleans, USA.

[17] S.G. Dhande, and J. Chackraborty, 1978, "Mechanical Error Analysis of Spatial Linkages", *ASME Journal of Mechanical Design*, Vol. 100, pp. 732 - 738.

[18] M. Mayourian, and J. Rastegar, 1990, "Stochastic Modeling of the Mechanical Behavior of Mechanisms in the Presence of Joint Clearances", *Proceedings of 1990 ASME Mechanisms Conference*, Chicago, USA, pp. 177 - 182.

[19] S. Li, Z. Xianmin, and J. Yang, 1998, "Error Transfer of Planar Linkages with Pair Clearance (Part I, the Error Transfer Coefficient of Experimental and Practical Mechanism)", *Proceedings of 1998 ASME Design Engineering Technical Conference*, Atlanta, USA, Paper MECH-5913.

[20] S. Dubowsky, M. Norris, M. Aloni, and A. Tamir, 1984, "An Analytical and Experimental Study of the Prediction of Impacts in Planar Mechanical Systems with Clearances", *ASME Journal of Mechanisms, Transmissions, and Automation in Design*, Vol. 106, No. 4, pp. 444 - 451.

[21] K. Soong, B.S. Thompson, 1987, "An Experimental Investigation of the Dynamic Response of a Mechanical System with Bearing Clearance", *ASME Advances in Design and Automation*, Vol. 10, No. 2, pp. 411 - 420.

[22] S. Dubowsky, 1974, "On Predicting the Dynamic Effect of Clearances in Planar Mechanisms", *ASME Journal of Engineering for Industry*, Vol. 93 B, No. 1, pp. 317 - 323.

[23] R. Wilson, and J.N. Fawcett, 1974, "Dynamics of the Slider-Crank Mechanism with Clearance in the Sliding Bearing", *Mechanism and Machine Theory*, Vol. 9, pp. 61 - 67.

[24] R.S. Haines, 1980, "A Theory of Contact Loss at Revolute Joints with Clearance", *Journal of Mechanical Engineering Science*, Vol. 22, No. 3, pp. 121 - 136.

[25] S. Dubowsky, and T.N. Gardner, 1975, "Dynamic Interactions of Link Elasticity and Clearance Connections in Planar Mechanical Systems", *ASME Journal of Engineering for Industry*, Vol. 97, No. 2, pp. 652 - 661.

[26] A.L. Schwab, J.P Meijaard, and P. Meijers, 2002, "A Comparison of Revolute Joint Clearance Models in the Dynamic Analysis of Rigid and Elastic Mechanical Systems", *Mechanism and Machine Theory*, Vol. 37, pp. 895 - 913.

[27] V. Parenti-Castelli and S. Venanzi, 2001, "A New Technique for Clearance Influence Analysis in Planar Mechanisms", *Proceedings of the 2002 ASME Design Engineering Technical Conference*, Montreal, Canada, Paper MECH-34318.

[28] F.L. Litvin, 1955, "Application of Matrices and Dual Number Calculations to Analysis of Spatial Gearings", *Proceedings of Leningrad Polytechnic Institute*, No. 182 (in Russian).

[29] J. Denavit and R.S. Hartenberg, 1955, "A Kinematic Notation for Lower Pair Mechanisms Based on Matrices", *ASME Journal of Applied Mechanics*, No. 22, pp. 215 - 221.

[30] L.W. Tsai, 1996, "Kinematics of a Three-Dof Platform with Three Extensible Limbs", Recent Advances in Robot Kinematics, (J. Lenarcic and V. Parenti-Castelli Eds.), Kluwer Academic Publishers, pp. 401 - 410.